

Earth Physics

Research into the structure and dynamics of the Earth uses a range of physical and mathematical techniques and is grouped into the three main themes of Seismology and Mathematical Geophysics, Geophysical Fluid Dynamics, and Geodynamics and Geodesy. The work spans observational, theoretical, laboratory, computational and data oriented studies, all directed towards understanding the structure and physical processes in the earth's interior, the crust or the earth's fluid envelope.

Two members of the Earth Physics academic staff received awards this year. Prof B.L.N. Kennett received the Gold medal in Geophysics from the Royal Astronomical Society, London, for his work in seismology and the Peter Baume Award from ANU for his exemplary record of research achievement and leadership. Prof K. Lambeck contributed to the award of the Nobel Peace Prize for 2007 to the Intergovernmental Panel on Climate Change (IPCC), as a substantial contributor to the IPCC since the inception of the organization.

PhD theses were submitted by T. Prastowo ("Mixing in buoyancy-driven exchange flows"), M. Coman ("Convective circulation forced by horizontal gradients in heating"), J. Dawson ("Satellite radar interferometry with application to the observation of surface deformation in Australia") and G. Estermann ("Contribution of mountain glacier melting to sea-level changes: Recent past and future"). New Postdoctoral academic staff commencing during 2008 include M. Ward in ocean modeling, S. Pozgay and A. Coffey in seismology, G. Luton on geodesy and S. Bonnefoy in computational geophysics.

RSES is taking a major role in Component 13 of the National Cooperative Research Infrastructure Strategy (NCRIS): "Structure and Evolution of the Australian Continent", which is managed through 'AuScope'. RSES hosts activities in Earth Imaging through support of portable instrumentation and transects, Geospatial through gravity measurements and testing of portable equipment for satellite laser ranging, and Simulation & Modelling through 'pPlates' software for tectonic reconstruction. As a linked activity between three AuScope components (Imaging, Geospatial and Access and Interoperability), the Terrawulf II cluster computer at RSES provides capability in geophysical inversion and the computation reduction of observational data.



Acting Director Prof. Ross Griffiths launching the Terrawulf II computational facility in June at RSES. TII is the latest in a long line of Geoscience computational facilities at RSES stretching back 30 years. Projects initiated in 2008 range from atmospheric effects in GPS, through ocean modeling to studies of the Earth core and geodynamo.

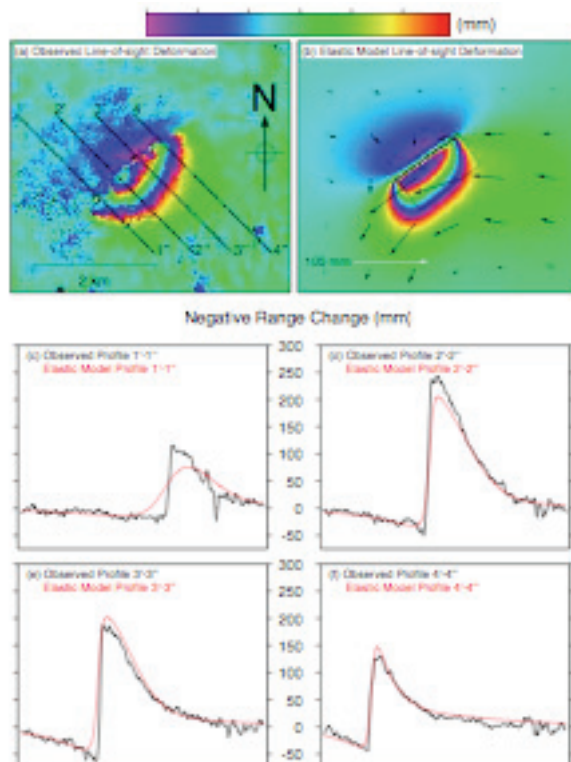
Centre for Advanced Data Inference

In the Centre for Advanced Data Inference a new, more powerful compute cluster, Terrawulf II, was commissioned early this year. The new cluster was made possible by NCRIS funding combined with support from RSES. Terrawulf II consists of 96 dual processor dual core 2.8GHz Opteron systems with 8GB of memory per node, connected with Gigabit Ethernet. Half of the nodes are also connected through higher bandwidth switches, which significantly extend the range of potential applications of the cluster to both 'tight' and 'loosely' coupled codes. The Terrawulf II cluster is integrated into the AuScope grid and used for a broad range of geoscience data processing as well as continuing development of state of the art inversion and data inference software.

Geodynamics and geodesy

The geodynamics group within Earth Physics is involved in the Geospatial component of AuScope. NCRIS funding in this strand has enabled investment in geodetic infrastructure throughout Australia, including three new Very Long Baseline Interferometry (VLBI) sites, a national Global Navigation Satellite System (GNSS), terrestrial gravimeters, a test of a mobile Satellite Laser Ranging (SLR) system and a contribution towards the new Terrawulf II compute cluster. Members of the geodynamics group are involved in the AuScope Executive Committee, the Geospatial Steering Committee as well as the gravity, VLBI and Grid Computing subcommittees charged directly with the acquisition and deployment of the infrastructure. The ANU component of the above equipment includes an FG5 absolute gravimeter (acquired in April 2008), a relative gravimeter (acquired in July 2008), a gravity technician and a SLR technician. Dr Jason Zhang, the SLR technician, was involved in instrument testing at Burnie, Tasmania early in 2008 while Mr Geoff Luton has been involved in FG5 observations in Melbourne, Hobart and Western Australia.

The InSAR analysis of small, shallow earthquakes in Western Australia demonstrated the capability of the technique to not only estimate fault plane location, orientation and depth but also to estimate the distribution of slip on the fault plane (Dawson et al., 2008). The stress drop for the Mw=4.7 Katanning earthquake was found to be 14-27 MPa, significantly smaller than expected for such a small event. This suggests that the seismic hazard of small earthquakes might be higher than previously thought.



Observed and modelled interferograms of deformation caused by the Katanning earthquake. Observed and modelled changes in round-satellite distance is shown across four different profiles (Dawson et al., 2008).

A combination of surface deformation from GPS and inferred deformation from changes in the Earth's gravity field from the Gravity Recovery and Climate Experiment (GRACE) have been undertaken to separate short-term hydrological variations from longer-term glacial isostatic adjustment as a result of melting of polar ice sheets since the Last Glacial Maximum. Coupled with continued advances in the analysis strategies of the raw GPS observations, these studies have revealed that both the GPS and GRACE estimates of surface deformation agree at the 1-2 mm level and mm/yr level, enabling highly accurate estimates of crustal deformation to be made.

Successful field experiments have been undertaken using the new gravimeters in Melbourne, Hobart and several sites in Western Australia. The GPS field programme in Papua New Guinea concluded this year while coral sampling in the Ningaloo Reef region continued in order to understand past levels of relative sea level.

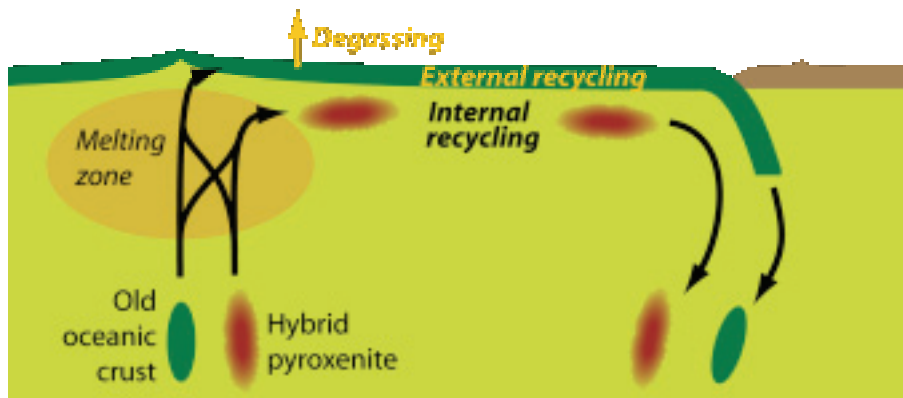
Geophysical fluid dynamics.

Highlights of work in geophysical fluid dynamics this year included laboratory and theoretical fluid dynamics studies modelling lava flows, where cooling, solidification and yield-strength are important factors. Experiments have focused on the flow of yield-strength fluid that is also cooling and solidifying as it flows down a sloping channel. A variety of inertial, viscous, plastic and cooling-controlled flow regimes have been found.

The geophysical fluid dynamics laboratory has also seen a renewed effort to understand the three-dimensional flow in mantle subduction zones, including the influences of an over-riding plate, back-arc spreading, the effects of a thick keel on the over-riding plate, and the behaviour of a hot mantle plume ascending under the over-riding plate. This work relied on an extended visit by Prof Kincaid and a student from the University of Rhode Island. The interaction of ascending mantle plumes and subduction zones is being examined with a view to explaining the distribution and ages of the Columbia River Basalts and volcanism of the Yellowstone hotspot. The work has shown that previously unsuspected patterns of volcanism can be produced and many aspects of the volcanism, including the age distributions, around Yellowstone and the Lava High Plains of the northwest USA can be explained by interaction of a plume and subduction zone.

Lessons learnt from several years of numerical modelling of the combined chemical and thermal evolution of the mantle are now bearing fruit in two directions. The models are being extended to Venus' mantle to test whether the 'basalt barrier' mechanism, reported last year, can explain the outburst of volcanism that completely resurfaced Venus about 500 Myr ago. Initial results are promising.

The insights from the numerical modelling have also fed into a new hypothesis to reconcile mantle chemistry with mantle dynamics. The idea is that only a fraction of the melt generated under a mid-ocean ridge actually reaches the surface. The remaining melt is trapped in the mantle, and carries the so-called incompatible elements. This hypothesis removes the need for a postulated deep, hidden reservoir containing 'missing' incompatible elements. It can also explain the presence of enigmatic 'unradiogenic' helium and other noble gases that emanate from some hotspot volcanos.



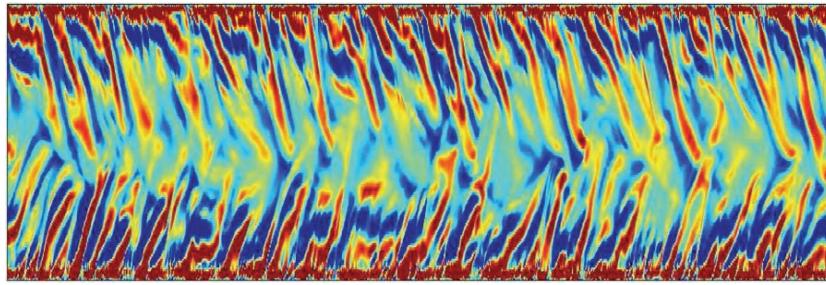
Cartoon of how noble gases may be partially retained in the mantle despite losses due to melting under mid-ocean ridges. Some of the melt is trapped, in the form of hybrid pyroxenite, and recycled internally without losing its gases. The melt that reaches the surface forms oceanic crust that degasses.

Studies of the fundamental dynamics of the ocean's meridional overturning circulation continued in the geophysical fluid dynamics laboratory. A new approach to the energetics of the circulation developed this year has elucidated the way in which energy supplied to irreversible turbulent mixing from the winds and tides must be in balance with the available potential energy supplied by the surface buoyancy fluxes. The two are closely tied, the buoyancy fluxes providing the driving force while the turbulent mixing maintains the stratification, and hence the strength of the forcing and the consequent rate of overturning. Numerical solutions have revealed the presence of significant internal gravity wave activity generated by the convection. It will require further work to determine whether there is likely to be substantial wave generation under oceanic conditions, and whether the wave energy can contribute to the vertical mixing. The steady-state dynamics were also examined in experiments with the case of a large ocean basin connected to a marginal sea by flow over a topographic sill. The exchange flow can influence the circulation and stratification in the ocean.



A video clip (available on-line) of flow in the laboratory convection model, in which the base is heated near both ends and cooled over the central half. The right hand section of the base is heated by an applied heat input 10% smaller than that applied to the left hand section of the base. Hence the plume at the left hand end is stronger than that at the right end and fills the top of the box. In the oceans this is analogous to the strongest sinking region producing the bottom waters.

In other experiments the response to small changes in the surface boundary conditions, such those as implied by global warming, has been investigated. The conditions leading to a potential shutdown of the deep sinking leg of the overturning circulation in simplified cases have been outlined. A first set of experiments with periodic oscillatory surface forcing is also providing insights into whether the global circulation is influenced by fluctuations having periods from the annual seasonal cycle (which is known to force variations in the deep sinking of cold waters) to millennia (which is the time scale for complete equilibration of the stratification to new surface conditions).

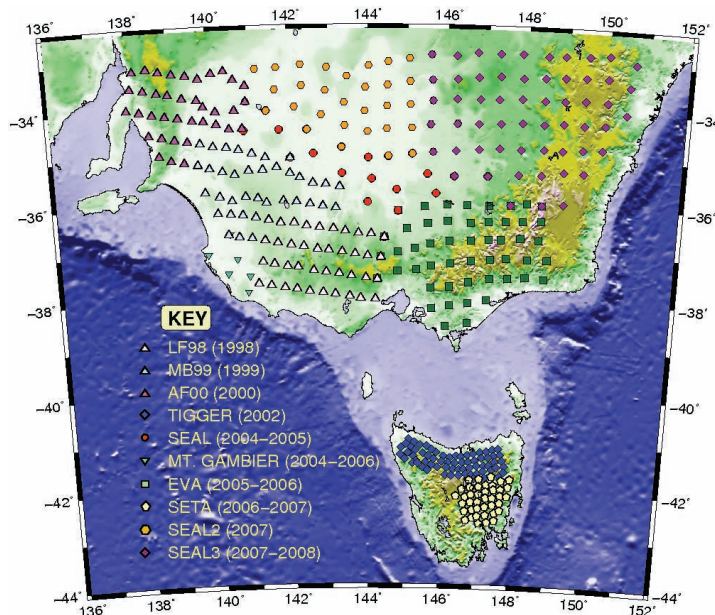


Hovmöller plot of the vertical velocity along a horizontal section at mid-depth from a 2-D numerical simulation of horizontal convection. Time increases upwards; blue represents upwelling motion, green approximately no motion, and red downwelling motion. Regions of high latitude sinking are situated in this case at both the left and right hand ends of the horizontal section, and excite strong wave modes that propagate towards 'low latitudes' at the centre of the section. These waves and their interactions appear to be responsible for much of the variability in the circulation.

In another laboratory study, the dynamics of wakes behind islands and headlands were shown to be sensitive to eddy disturbances or turbulence carried from upstream of the topographic feature. The incident disturbances cause a faster dissipation of wake instabilities with distance downstream, hence a smaller recirculation region. This study is currently being extended to a practical application involving the dispersion of wastewater released into a major estuary in which there is a separation of the flow in the main channel and a relatively slow flushing of a shallow region to one side. Preliminary experiments in a water flume are exploring the roles of wastewater outflow location and tides on the flushing time.

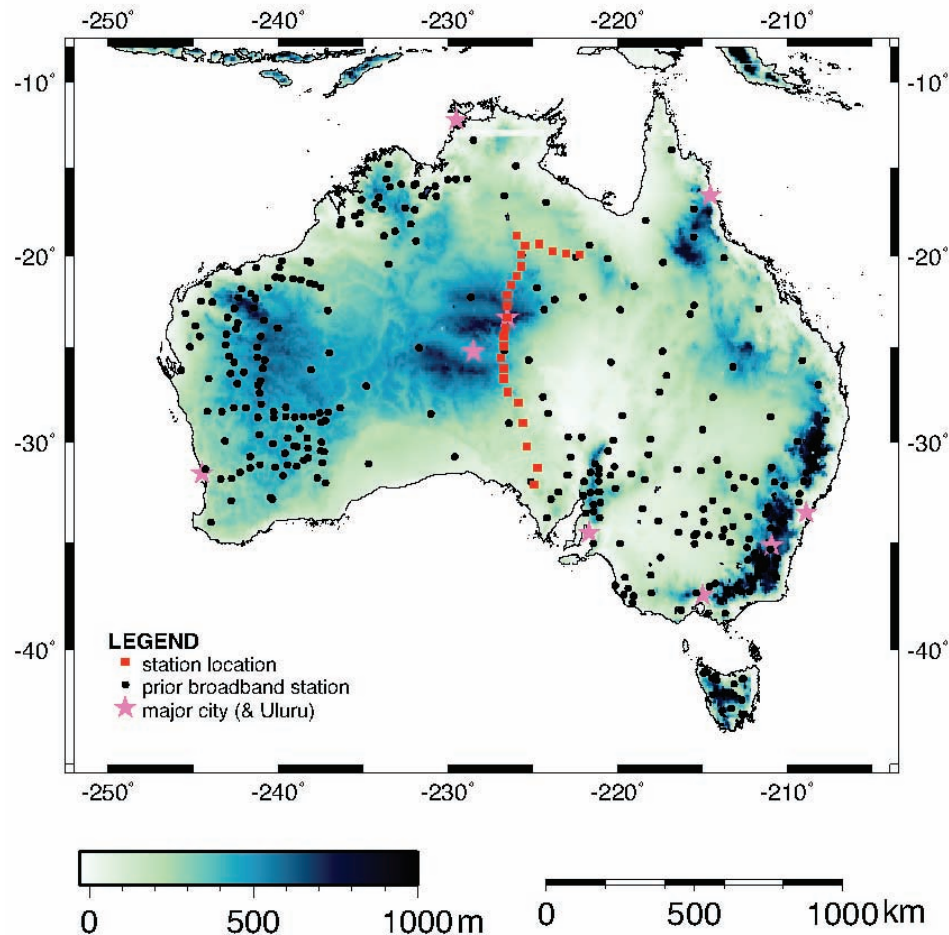
Seismology.

2008 was an eventful year for seismic experiments, with the deployment of two new arrays, and the continued maintenance of the SEAL3 array which was deployed in late 2007. SEAL3 comprises 57 3-component short period stations distributed throughout southeast New South Wales at a spacing of approximately 50 km. With a recording period in excess of 1 year, this study has substantially contributed to the cumulative coverage of passive seismic data in southeast Australia. To date, nearly 400 sites have been occupied in Tasmania, Victoria, South Australia and New South Wales. Teleseismic tomography, ambient noise tomography, receiver functions and core phase studies are currently in progress using SEAL3 and pre-existing data.



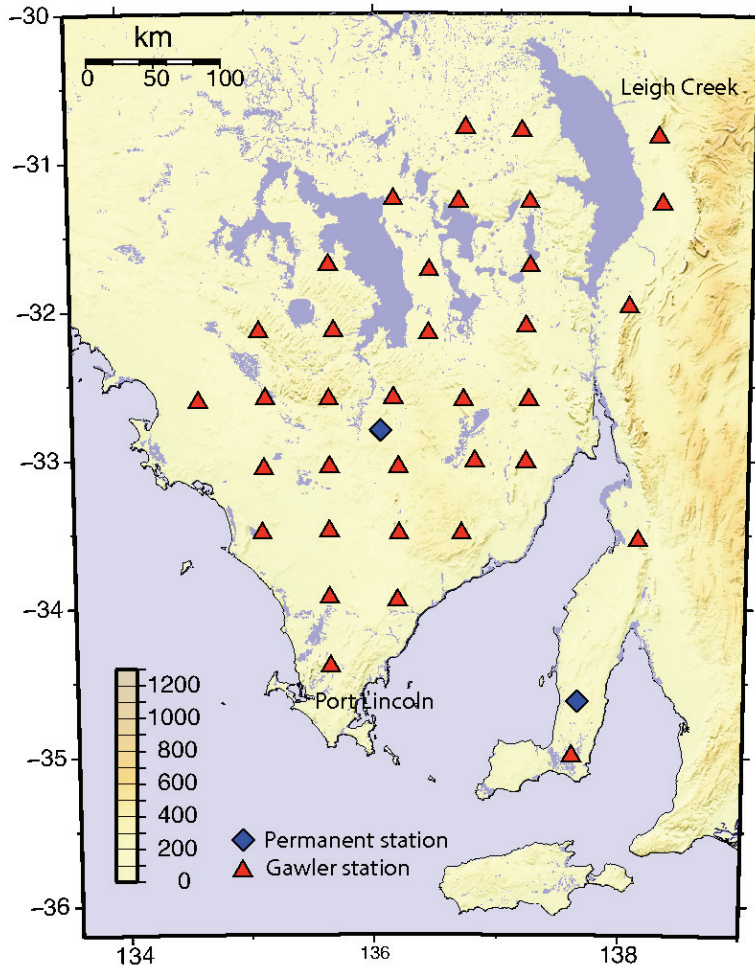
Location of all short period seismic arrays deployed in southeast Australia over the last 10 years.

In order to determine the nature of the transition at lithospheric depths between the northern and southern Australian cratons, a transect of 25 broadband seismic stations was deployed between the Eyre Peninsula in South Australia and Tennant Creek in the Northern Territory. The installation took place in August-September 2008, with all stations expected to remain in operation for at least one year. With a site spacing of between 60-90 km, receiver functions, shear wave splitting and travelt ime inversion can be utilized to help address fundamental questions relating to the anomalously slow velocities beneath the central Australian intercratonic structures, and how they propagate with depth.



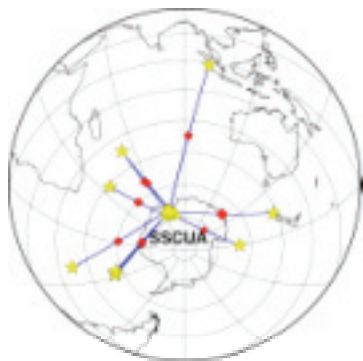
Bilby array comprising 25 broadband seismometers deployed in central Australia.

In June-July 2008, an array of 35 short period seismometers was installed across the Gawler Craton in South Australia for an eight month period. Station spacing is approximately 50 km and the area covered runs from Port Lincoln in the Eyre Peninsular to Leigh Creek just west of the Flinders Ranges. The primary aim of this array is to increase passive data coverage in this part of Australia for seismic imaging, which includes teleseismic tomography and receiver function analysis. Local earthquakes, which are relatively plentiful in this part of Australia, will also be exploited to improve structural constraints. The eastern edge of the Gawler craton is currently of particular interest for the supply of geothermal energy and there are many ongoing industry projects in the area. Geoscience Australia completed a deep seismic reflection transect across the top of the Eyre Peninsular just prior to the deployment of the Gawler array. This array will provide broad scale earth imaging required for more detailed studies.



Short period array deployed across the Gawler craton in mid 2008.

In 2008 the conversion of a large portion of our seismic data from past experiments to an international standard format called "miniseed" was accomplished. This is the first step in building a continuous archive of data, which is now easily accessible by local researchers through a java acquisition tool called Seismic Data Centre (SDC). About one half of our data has been converted and it is a work in progress. In other projects it was shown that it is not feasible to use 1D structural model for Australia when inverting for source parameters of large earthquakes surrounding Australia, and that a 3D model will be needed for the computation of Green's functions. This work is important in the context of the Tsunami warning for Australia. Work also commenced on the lithospheric structure of the Balkans peninsula using receiver functions, and an interactive tool (java) for forward modelling of receiver functions was completed. A large dataset from Antarctica was used to examine current hypotheses about the core anisotropy and structure showing in particular that the Antarctic data do not support the existence of significant heterogeneity in the outer core Taylor cylinder.



Distribution of events (stars) with clear PcP arrivals recorded at SSCUA stations in Antarctica (triangles). The red diamonds are bouncing points of the PcP waves at the CM

Ambient noise tomography in Southeast Australia

Pierre Arroucau¹, Nick Rawlinson¹ and Malcolm Sambridge¹

¹ *Research School of Earth Sciences, Australian National University, Canberra, ACT 0200, Australia*

Previous studies have demonstrated that the Green's function of the medium between two stations can be extracted from the cross-correlation of the seismic ambient noise wavefield recorded at these stations. This class of technique is now progressively becoming a standard seismic investigation tool and has successfully been used for tomographic imaging purpose in many parts of the world. Saygin (2007) obtained encouraging results for the Australian continent using broadband records, and showed that Rayleigh wave group velocity contrasts within Australia correlated well with its major geological units.

In the last decade, dense rolling short-period seismic array deployments have been carried out by RSES in Southeast Australia (WOMBAT-SE). With an interstation distance of a few tens of km, several months of continuous records and a cumulative total of approximately 400 stations, these temporary arrays provide an unique opportunity for high-resolution ambient noise imaging in the region, which can address fundamental questions regarding the structure and tectonic evolution of the Lachlan and Delamarian orogens, which underpin the southern half of Palaeozoic eastern Australia.

Dispersion curves constructed from the cross-correlation of the vertical component, by means of frequency-time analysis for periods ranging between 1 to 20s, have been used to extract Rayleigh wave group traveltimes. An iterative non-linear tomographic scheme based on the fast marching method, a grid-based eikonal solver, and a subspace inversion method, was used to map the traveltimes as variations in Rayleigh group wavespeeds at different frequencies.

Saygin, E, (2007) Seismic Receiver and Noise Correlation Based Studies in Australia. *PhD Thesis, The Australian national university*, 175p.

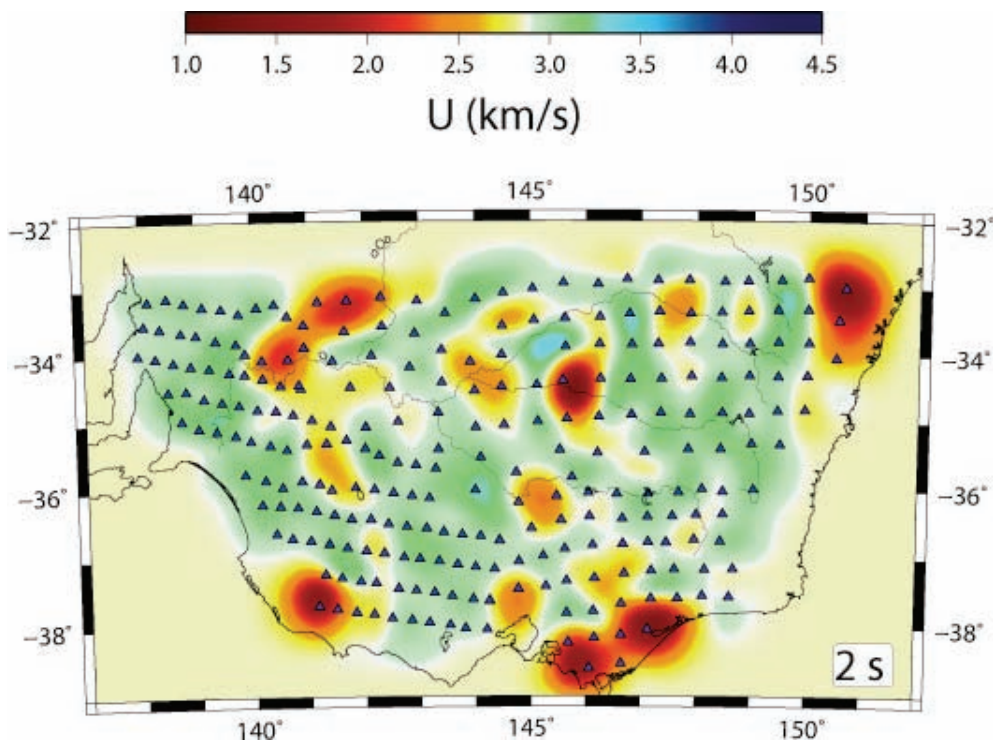


Figure 1. 2-second Rayleigh wave group velocity in Southeast Australia obtained from ambient noise cross-correlation of the vertical component for simultaneously recording pairs of stations. The stations used belong to 10 temporary arrays of short-period instruments deployed in the last decade.

Seismic Tomography With a Transdimensional Markov Chain

Thomas Bodin, Malcolm Sambridge¹

¹ *Research School of Earth Sciences, Australian National University, Canberra, ACT 0200, Australia*

In seismic tomography, the Earth's interior must be parametrized in some fashion. This is typically done using uniform local cells, and the inversion process consists of finding seismic wave speeds within each cell. The number of cells (and size) has to be chosen according to a compromise between model resolution and model uncertainty. Usually, seismologists choose to have a large number of cells and then face the problem of non-uniqueness by imposing constraints on the solution that are independent of the observations, i.e. by employing regularization procedures like spatial smoothing and norm damping. The type and weighting applied to regularization terms often forms a subjective choice of the user. Another aspect is that the strength of damping and smoothing is determined globally which raises the possibility that, while the ill-constrained regions are being suitably damped, the well constrained regions may be over-smoothed with resulting loss of information from the data.

Our work this year has been devoted to using some new ideas in nonlinear inversion to determine the model dimension (i.e. the number of cells) during the inversion. Treating the number of unknowns as an unknown itself has received little attention in geophysics. However, for more than 10 years, Markov chain Monte Carlo (MCMC) methods that admit transitions between states of differing dimension have been actively developed in the area of Bayesian statistics.

We have developed an approach which uses Voronoi cells instead of a regular mesh for an Earth parametrization (see Figure 1). The Voronoi cells are defined by their centres which are able to move. That is, the number and the position of the cells defining the geometry of the velocity field, as well as the velocity field itself are unknowns in the inversion. The inversion is carried out with a fully non-linear parameter search method based on a trans-dimensional Markov chain.

At each step of the chain, a change from the current model is proposed : we either change the velocity or the position of one random cell. The algorithm also allows jumps between dimensions by adding or removing random cells. The forward problem is computed and provides new estimated travel times. The new misfit to observed travel times is compared to that of the current model. The proposed model is either accepted or rejected using a predefined probabilistic threshold.

The Markov chain produces an ensemble of models with different dimensions which carries relevant statistic information about the unknown velocity field. The method takes as a solution the average of this family of models. Each model in the ensemble has a different parametrization but the average is continuous without obvious 'parametrization' artefacts. The standard deviation of the ensemble forms a continuous map and can be used as a proxy for the error for the solution model.

The method has been tested on synthetic situations where the ray coverage is not uniform and where the parametrisation is an issue (see Figure 2). A major advantage is that explicit regularisation of the model parameters is not required, thus avoiding global damping procedures and the need to find an optimal regularisation value. The technique has also been tested on real data and gives promising results.



Figure 1: Voronoi cells about 30 pseudo random points on the plane. The cell nuclei have been drawn from a 2-D uniform distribution over the spatial domain delimited by the red rectangle. The cell boundaries are defined as the perpendicular bisectors of pairs of nuclei. Any point inside a cell is closer to the nucleus of that cell than any other nucleus.

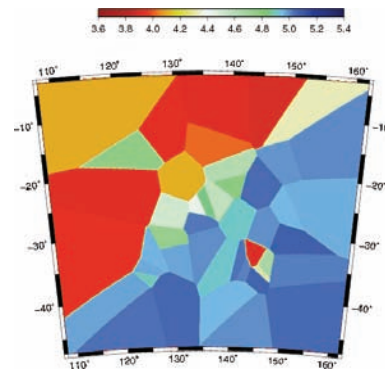
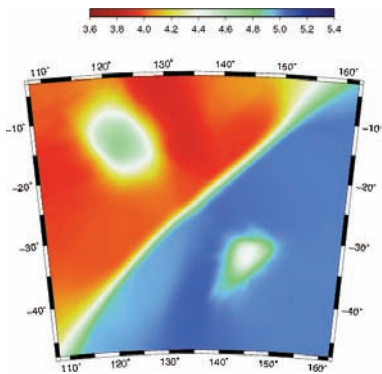
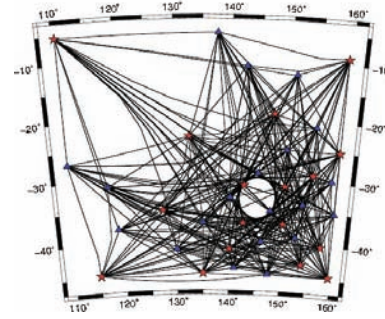
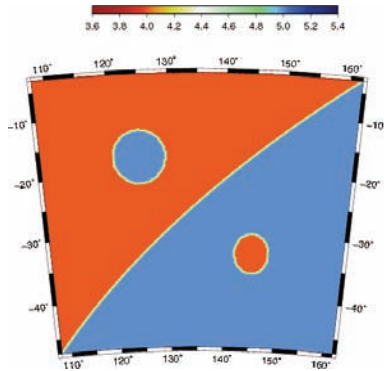


Figure 2 : Upper left map shows the true model. The upper right map shows the ray geometry. The lower left map shows the model sampled with the best fit to the data and the lower right map shows the average estimated solution.

Terrawulf II

Malcolm Sambridge¹, Herb McQueen¹, Shinta Bonnefoy¹

¹ *Research School of Earth Sciences, Australian National University, Canberra, ACT 0200, Australia*

TerraWulf is a networked cluster of computers set up in RSES to provide convenient high end computing power for a range of demanding geoscience problems. A major upgrade of the TerraWulf compute cluster was recently made possible by funding support from the National Collaborative Research Infrastructure Strategy (NCRIS) under the AuScope umbrella. Contributions from the AuScope Geospatial, Imaging and Structure, and Access and Interoperability components combined with support from RSES have enabled the construction of a new and more powerful cluster. The hardware was delivered and assembled in 2007 and commissioning and benchmarking continued through the first half of 2008.

On Friday 27th June 2008 TerraWulf II was launched at the Research School of Earth Sciences by Acting Director Prof. Ross Griffiths. It has a total of 24 Tb of disk storage and 1Tb of RAM and was built to tackle large complex computational problems in the Earth Sciences using parallel processing techniques. 'TII', is the latest in a long line of Geoscience computing platforms at the RSES which stretch back more than 30 years. Projects initially identified for TII include applications in seismic imaging of Earth structure, geospatial data analysis and mathematical geophysics. TII is open for access by the Australian Earth Science community for projects consistent with the AuScope vision to '...characterise the structure and evolution of the Australian continent from surface to core in space and time.' It is accessible directly through a local account and via the AuScope grid.

The main cluster consists of 96 nodes (384 processor cores) connected through Gigabit and Infiniband switches which support a range of potential applications of the cluster including both 'tight' and 'loosely coupled' codes. Each node is an IBM System x3455 with 2 AMD Opteron Dual-core 2.8 GHz processors, 160 GB local disk and 9GB to 17GB RAM. All the nodes are interconnected through SMC8848 Gigabit Ethernet switches, and half of the cluster is also inter-connected via three 24port Voltaire ISR9024S Infiniband switches providing 10Gbit inter-process communication. Compute nodes are configured with Open SUSE 10.3 and two kinds of MPI environment, MPICH2 and VLTMPI, have been installed to enhance paralalled processing applications. It is accessible directly through a local account and via the AuScope grid.

The TerraWulf II cluster is now running a variety of geoscience data processing, technique development, simulation and analysis codes. Current projects include studies of atmospheric effects in GPS analysis, ocean overturning circulation and Earth's inner core structure & geodynamo, as well as multi-arrival wavefront tracking seismic tomography, inversion of airborne electromagnetic data, development of nonlinear inversion methods, implementation of earthquake source parameter inversion, and high-resolution ambient noise tomography.



Figure 1.

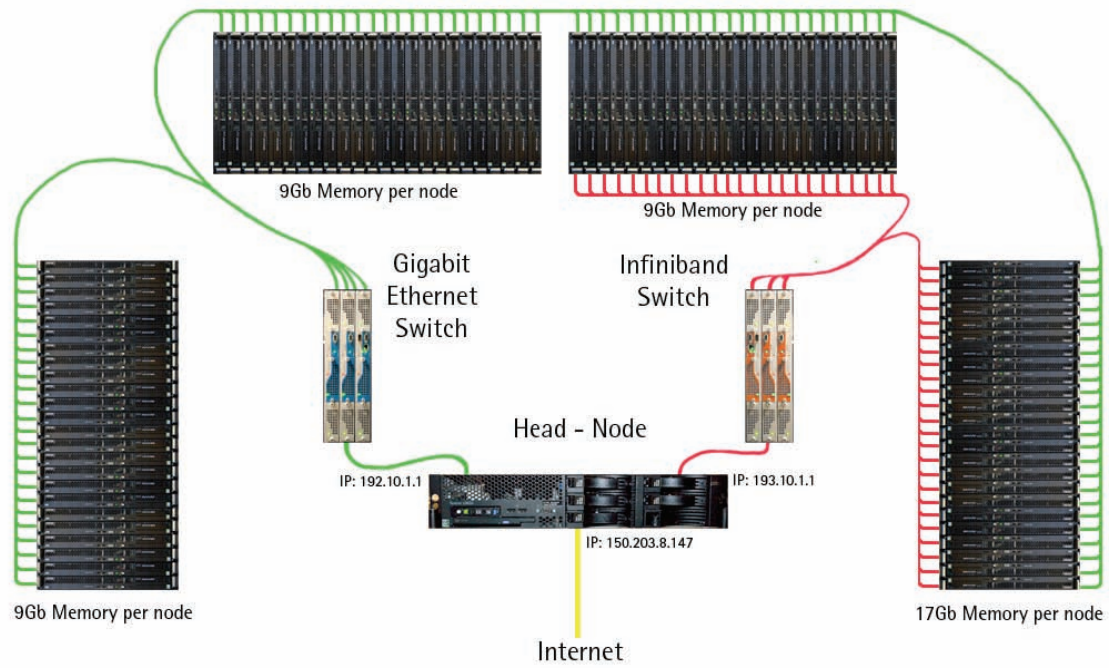


Figure 2.

Holistic inversion of time-domain airborne electromagnetic data

Ross Brodie¹ and Malcolm Sanbridge¹

¹ *Research School of Earth Sciences, Australian National University, Canberra, ACT 0200, Australia*

Since the research on this project resumed in August 2008 we have been investigating the feasibility of applying our holistic inversion technique to time-domain airborne electromagnetic (AEM) data. Holistic inversion was originally developed to invert frequency-domain AEM data to solve for continuous 3D survey wide conductivity model while simultaneously solving for systematic calibration errors (e.g., scaling effects, phase shifts and zero-level bias) which often degrade frequency-domain data (Brodie and Sanbridge, 2006).

One of the challenging 'calibration' issues in fixed-wing time-domain AEM is the fact that the position and attitude of the receiver coils, which are towed ~120m behind and ~40m below the aircraft, cannot be accurately measured under normal operating conditions. This receiver geometry information is a critical input into quantitative modelling and inversion routines. Conventionally the receiver coils' position are estimated from the measured AEM data during the routine data processing. However this requires assumptions to be made about the conductivity of the subsurface and the attitude of the receiver coils. When these assumptions are poor the estimated receiver position is not accurate, which results in the data not being able to be fitted and/or inaccurate conductivity models being estimated from subsequent inversions. More recently it has been demonstrated that a better approach is to simultaneously invert for the system geometry and the conductivity model (Lane et al., 2004).

The fixed-wing time-domain holistic inversion we improve on this by inverting not just one sample of AEM data at a time but a whole flight line of data. Figure 1 shows a schematic outline of the elements of the inversion formulation. We solve for layer conductivities, the transmitter to receiver in-line (D_x) and vertical separations (D_z), and the receiver pitch (R_p). All of these are parameterized as along line 1D cubic B-splines. Splines are an ideal choice because they are able to naturally represent the smooth and continuous along line variation of receiver geometry that occurs in reality. In doing so we are able to exploit the along line coherency, which is not accessible to the conventional sample by sample inversion, to improve upon the accuracy and stability of the inversion.

As a demonstration of the improvement that the new method offers, we have inverted a flight line of data that was acquired with the TEMPEST system using the two techniques. Figure 2 shows the results using a conventional inversion in which we solve for the layer conductivities independently for each airborne sample point and stitch the results together post-inversion to form a conductivity section. We did not solve for the receiver geometry. Figure 3 shows the results for the holistic method where we inverted the whole line at once to solve for the layer conductivities and three receiver geometry parameters, each parameterized as along line splines.

In the holistic inversion the data was able to be fitted to the expected misfit value of 1. However they were not able to be fitted in the conventional inversion due to inaccurate receiver geometry estimates made during the data processing. The holistic inversion conductivity section does not have the numerous vertical artefacts that are apparent in the conventional inversion section. This makes it more geologically realistic and continuous, and thus easier to interpret/trace subtle features. As a means of gauging the relative accuracy of the methods via independent ground truth two downhole conductivity logs (GW800232 and LMQ03) are plotted over the conductivity sections in the same color lookup scheme. It can be seen that in the vicinity of both logs the holistic inversion more accurately reproduces the downhole logs.

Brodie RC, Sambridge M (2006) A holistic approach to inversion of frequency-domain airborne EM data. *Geophysics* 71: G301–G312

Lane R, Brodie RC, Fitzpatrick A (2004) Constrained inversion of AEM data from the Lower Balonne Area, Southern Queensland, Australia. *CRC LEME open file report* 163

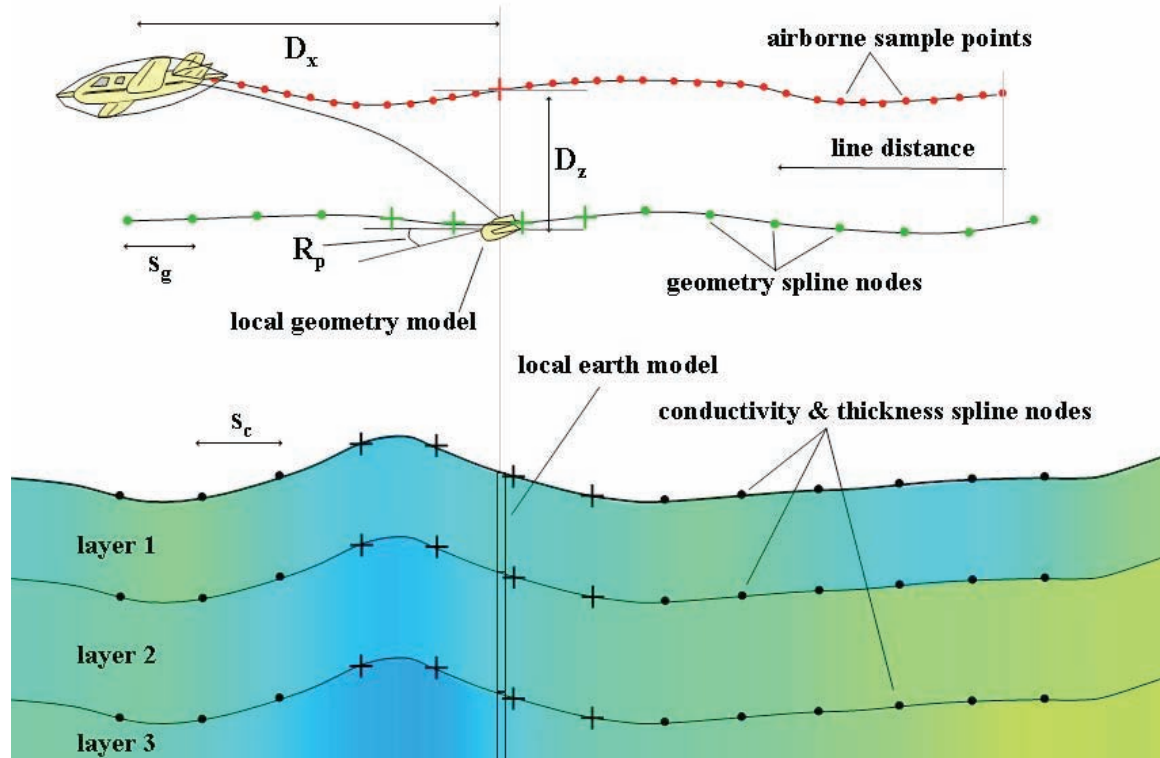


Figure 1.

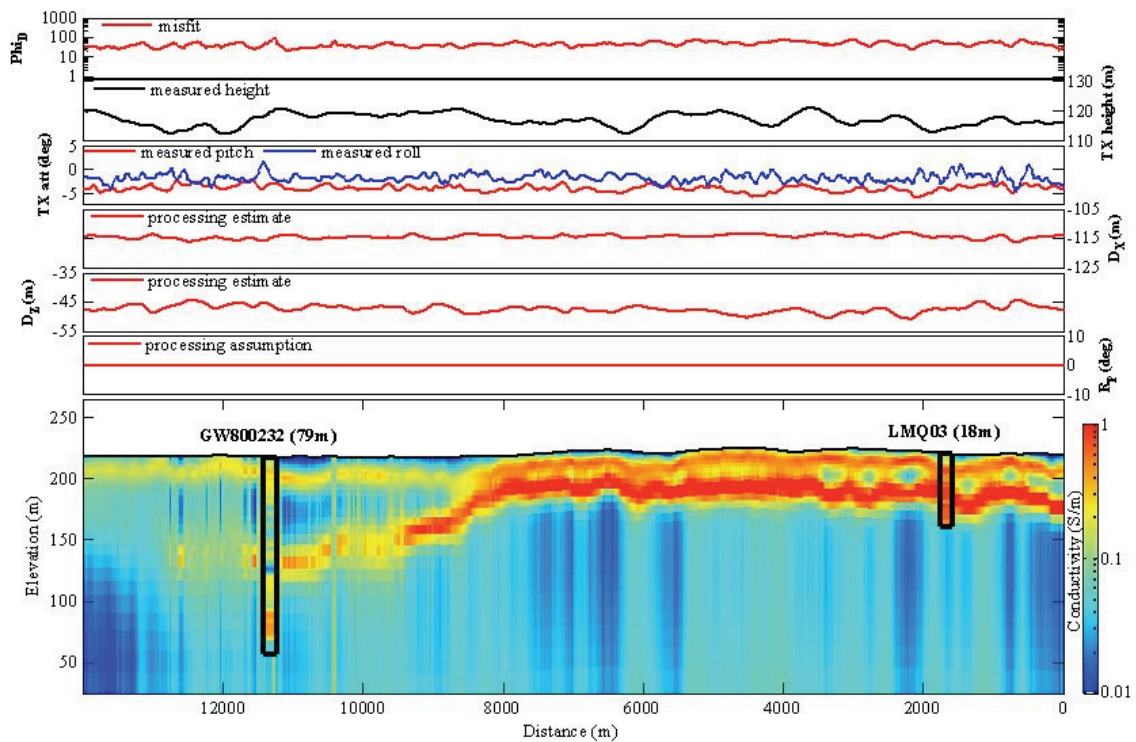


Figure 2.

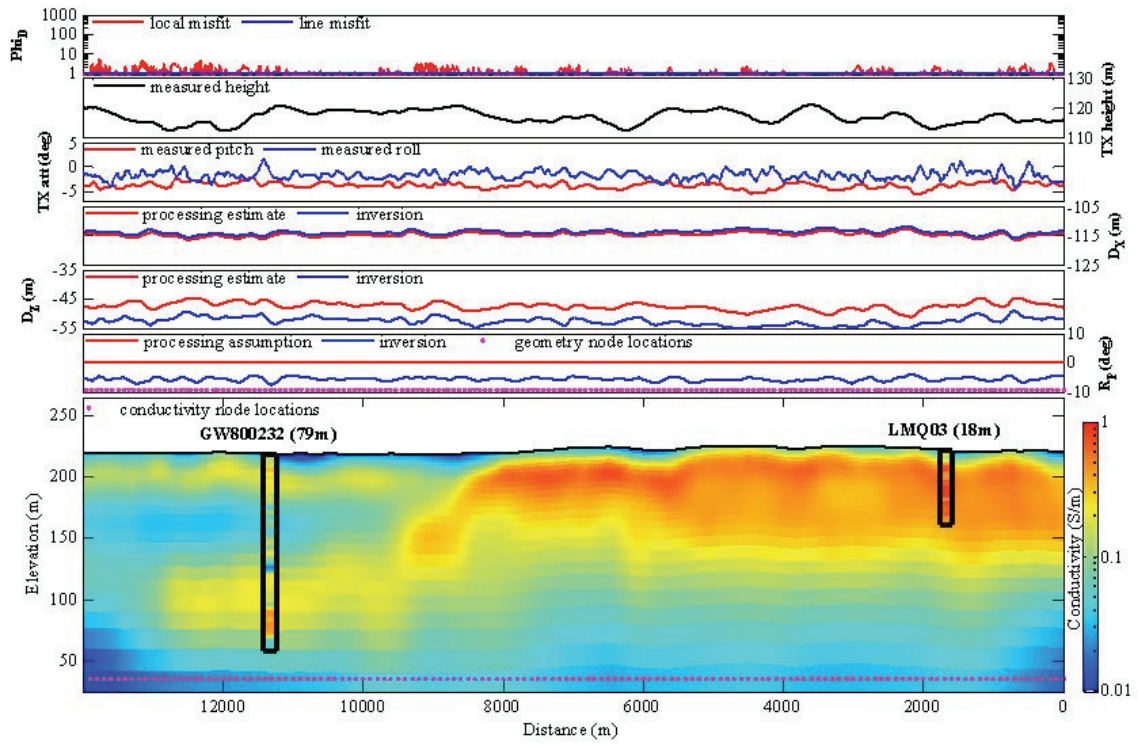


Figure 3.

Mantle Evolution, Dynamical and Chemical, Earth and Venus

Geoffrey F. Davies and Andreea Papuc

Research School of Earth Sciences, Australian National University, Canberra, ACT 0200, Australia

Numerical modelling of mantle dynamics is leading to important insights into the history of Earth and Venus.

A series of studies of how mantle convection stirs chemical tracers has established a quantitative basis for a new hypothesis regarding the abundance of trace elements in the mantle, including the enigmatic noble gases. Because the mantle is heterogeneous, being a mixture of subducted oceanic crust and peridotitic mantle, the extraction of melt at mid-ocean ridges is expected to be inefficient. A cartoon of melting under ridges is shown in the Figure. The inefficient extraction implies that the abundance of incompatible trace elements in the mantle is higher than has been estimated in the past. Geophysical constraints indicate the abundance is 2-3 times previous estimates. This removes the need for a 'hidden' reservoir, clarifies the relationship between continental crust and the mantle, and helps to resolve a discrepancy between estimates of radioactive heating and models of the thermal evolution of the mantle.

The source of 'unradiogenic' helium, i.e. helium that has a low $^4\text{He}/^3\text{He}$ ratio, from Hawaii and other hotspots has been an enduring puzzle for which the new hypothesis offers a resolution. Melting of the heterogeneous mantle is expected to produce a 'hybrid pyroxenite' that contains much of the mantle's complement of incompatible elements, including the noble gases. It is also likely to be denser than average mantle, like subducted oceanic crust. Numerical models have shown that such denser components tend to partially settle to the bottom, plausibly explaining the seismological D" region at the base of the mantle. Whereas subducted oceanic crust is expected to contain little noble gas, the hybrid pyroxenite should contain substantial noble gas. Furthermore the material in D" has a longer residence time, according to the numerical models, so it will degas more slowly, meaning the content of primordial ^3He will be higher. D" is already believed to be the source of mantle plumes, so the new hypothesis offers a straightforward explanation of mantle helium observations. A simple quantitative model, based on results from numerical models, then successfully explains the helium, neon and argon observations from mid-ocean ridge basalts and oceanic island basalts.

These results, if substantiated, go far to reconciling mantle geochemistry with the dynamical picture of the mantle based on geophysical evidence and numerical modelling. It has been unclear for at least three decades how this could be achieved.

Work reported last year on numerical models that yield episodic layering and overturns in Earth's early mantle is now being extended to Venus. Venus was volcanically resurfaced about 500 Myr ago. PhD student Andreea Papuc's project is to investigate whether conditions in Venus' mantle today are conducive to layering and overturn, as Earth's mantle was early in Earth history. Layering occurs because of the 'basalt barrier' mechanism, in which subducted oceanic crust tends to accumulate at 660 km depth because it is buoyant between 660 and 750 km depth, but negatively buoyant at other depths. Initial results show that overturns are indeed still likely in Venus, mainly because of its hotter surface and lack of plate tectonics. Venus' slightly smaller size, gravity and mantle density also seem to favour layering, though it is not yet clear why. The effects of different lithosphere strengths are yet to be investigated, and the goal is to do evolutionary models of Venus. It will be important for understanding Venus' atmosphere and geochemistry to know whether and how often earlier resurfacing events might have occurred.

Davies, G. F. (2008) Inefficient melt extraction from a heterogeneous, mildly depleted mantle: no hidden reservoir, *Earth Planet. Sci. Lett.*, submitted.

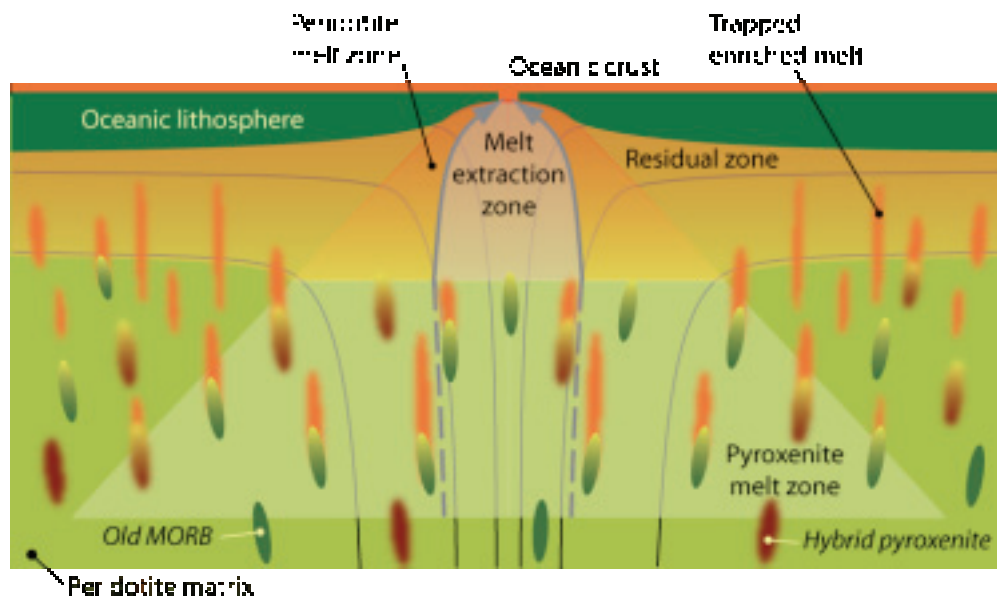


Figure 1. Melting under a mid-ocean ridge in a heterogeneous mantle.

Detecting Australian Earthquakes with InSAR

John Dawson^{1,2} and Paul Tregoning¹

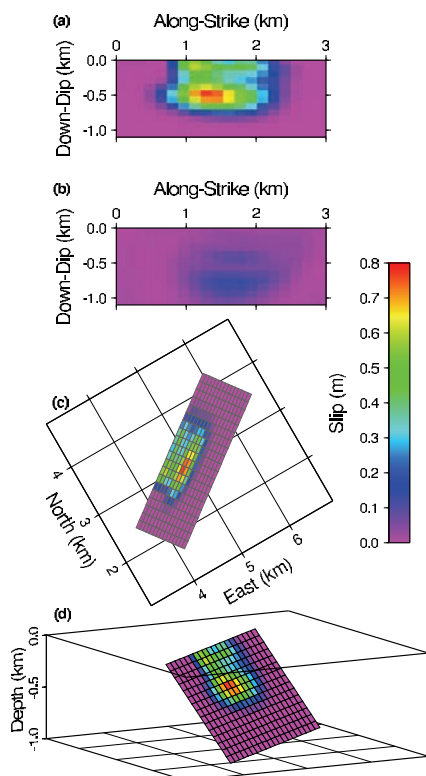
¹ Research School of Earth Sciences, Australian National University, Canberra, ACT 0200, Australia

² Geoscience Australia, Canberra, Australia.

Analysis of Interferometric Synthetic Aperture Radar (InSAR) images has detected two shallow, intraplate earthquakes over the past three years. Each of these small earthquakes occurred in the top ~ 1 km of the crust and caused sufficient surface deformation that the location and fault parameters (orientation, dip, slip direction) could be estimated. These are the smallest magnitude earthquakes ever imaged by the InSAR technique (Dawson et al., 2008).

The Mw 4.7 October 2007 Katanning earthquake ruptured ~ 1 km² with an average slip of ~ 42 cm. This implies a static stress drop of 14–27 MPa which is much higher than previously expected for such a small event. The quality of the InSAR deformation estimates is sufficiently high that the depth of the event can be estimated with a precision of ~ 10 m. It was even possible to invert for the distribution of slip on the fault plane – the first time that this has been achieved for such a small event. These results have been published by Dawson et al. (2008).

The fine spatial resolution and accuracy that InSAR analysis can provide to the study of earthquakes in Australia opens up exciting new possibilities. Given the vastness of the Australian continent, it is likely that most earthquakes will not occur close to a seismic station. Therefore, the accuracy with which seismic data can be used to locate earthquakes is limited. Given that InSAR observations are made remotely from space platforms, the deformation from any shallow earthquake (ie < 5 km depth) can be captured by InSAR provided an image of the region exists prior to the earthquake. It is even conceivable that the highly accurate locations estimated by InSAR could be used as constraints in seismic inversions for crustal rheology modelling and/or as master event locations in a bootstrapping process to relocate other Australian earthquakes.



Dawson, J., P. Cummins, P. Tregoning, and M. Leonard, 2008. Shallow intraplate earthquakes in Western Australia observed by InSAR, *J. Geophys. Res.* 113, B11408, doi:10.1029/2008JB005807.

Figure 1. Slip distribution estimate of the Katanning earthquake, October 2007. A) Estimated slip. View is normal to the fault plane. b) 1_σ uncertainties of the slip. c) Plan view of the rupture in an arbitrary local coordinate system. d) Viewing azimuth and elevation is 210° and 10°, respectively (Dawson et al., 2008).

Relative sea-level changes due to ocean bottom pressure changes caused by thermal expansion

Gisela Estermann^{1,2}, Kurt Lambeck^{1,2} and Herb McQueen¹

¹ *Research School of Earth Sciences, Australian National University, Canberra, ACT 0200, Australia*

² *Antarctic Climate & Ecosystems, Cooperative Research Centre, Hobart, Tasmania 7001, Australia*

Ocean thermal expansion does not alter the total global ocean mass but can nevertheless result in relative sea-level changes. The heat uptake by the ocean (in the case of a warming climate) varies locally both horizontally and in depth. In a simplified model the total water column in the deep ocean tends to expand more than in shallow areas (illustrated with arrow 1 in Figure 1). In order to maintain an equipotential surface, water has to flow from the deep ocean to the shallow areas. This redistribution of water (illustrated with arrows 2 in Figure 1) consequently results in a spatial change in ocean bottom pressure. These ocean bottom pressure changes result in relative sea-level changes.

Atmospheric CO₂ concentrations and projected global sea-level rise over the period from 1860 to 2200 used here are based on IPCC scenario simulations (see Figure 2 in Landerer et al., 2007). Landerer et al. (2007) calculated ocean bottom pressure changes caused by secular oceanic mass redistribution due to thermal expansion. They developed a numerical model for the mass transfer from deep open water to coastal (shallow) areas. A data set of ocean bottom pressure changes produced by this model has been provided by Felix Landerer. The variations are expressed as changes of mass load in meters of water and are given on an annual basis from 1860 to 2200 on a 1° x 1° grid. Three examples of 10-year averages are shown in Figure 2. The plots show an increase in intensity of the redistribution of mass particularly from 2000 onwards.

The plots in Figure 2 show the overall transfer of mass from the southern to the northern hemisphere. In particular, the Arctic Ocean shelves experience an above-average increase in mass load. It appears that there is a good correlation between ocean bottom pressure changes and ocean bathymetry. For the IPCC scenario simulations used here, positive loads of up to 0.4 m by the end of the 21st century and 0.8 m by the end of the 22nd century are projected mostly for the Arctic Sea, while the deeper oceans (especially in the southern hemisphere) experience negative loads of -0.2 m and -0.4 m by 2100 and 2200, respectively. These results represent the redistribution of mass assuming a rigid Earth. Hence, the so-called second order relative sea-level changes as a result of the viscoelastic response of the Earth to the redistribution are now calculated. Since only thermal expansion is considered here, no mass is added or taken away from the ocean and the total change in mass over the oceans is zero.

The bottom pressure changes, expressed as water-mass loads, have been implemented in a sea-level program (the *calsea* program; Johnston 1993a,b; Lambeck et al., 2003). The resulting relative sea-level changes for 10-year averages are shown in Figure 3. Changes in relative sea level from this source are negligible until the beginning of the 21st century. By the end of the 22nd century, relative sea-level rise reaches a maximum of approximately 60 mm in the Arctic. This value is expressed relative to the mean of the period 1860-1869, which is assumed to be an unperturbed period. As the spatial distribution of relative sea-level changes (Figure 3) correlates with the spatial distribution of ocean bottom pressure changes (Figure 2), a rise in second order relative sea level is predicted mostly in coastal areas, in particular in the Arctic Ocean, whereas second order relative sea level falls in deep ocean areas.

Assuming this climate scenario adequately represents future thermal expansion, relative sea-level changes due to the redistribution of water caused by secular ocean mass redistribution are amplified by about 10% due to these ocean bottom pressure changes.

While there is a variety of uncertainties in thermal expansion models (e.g. size of the surface warming, the effectiveness of heat uptake by the oceans for a given warming, and the expansion resulting from a given heat uptake; see Section 11.5 in Church et al., 2001), predicted future sea-level changes will have to be increased by 10% to account for the redistribution of ocean water following thermal expansion.

Church, J. A., Gregory, J. M., Huybrechts, P., Kuhn, M., Lambeck, K., Nhuan, M. T., Qin, D., and Woodworth, P. L. (2001). Changes in Sea Level. In Houghton, J. T., Ding, Y., Griggs, D. J., Noguer, M., van der Linden, P. J., Dai, X., and Johnson, C. A., editors, *Climate Change 2001: The Scientific Basis. Contribution of Working Group I to the Third Assessment Report of the Intergovernmental Panel on Climate Change*, chapter 11. Cambridge University Press, Cambridge, United Kingdom and New York, NY, USA.

Johnston, P. (1993a). Deformation of the earth by surface loads. PhD thesis, The Australian National University, Canberra.

Johnston, P. (1993b). The effect of spatially non-uniform water loads on prediction of sea-level change. *Geophysical Journal International*, 114, 615–634.

Lambeck, K., Purcell, A., Johnston, P., Nakada, M., and Yokoyama, Y. (2003). Water-load definition in the glacio-hydro-isostatic sea-level equation. *Quaternary Science Reviews*, 22, 309–318.

Landerer, F. W., Jungclauss, J. H., and Marotzke, J. (2007). Ocean bottom pressure changes lead to a decreasing length-of-day in a warming climate. *Geophysical Research Letters*, 34 (L06307).

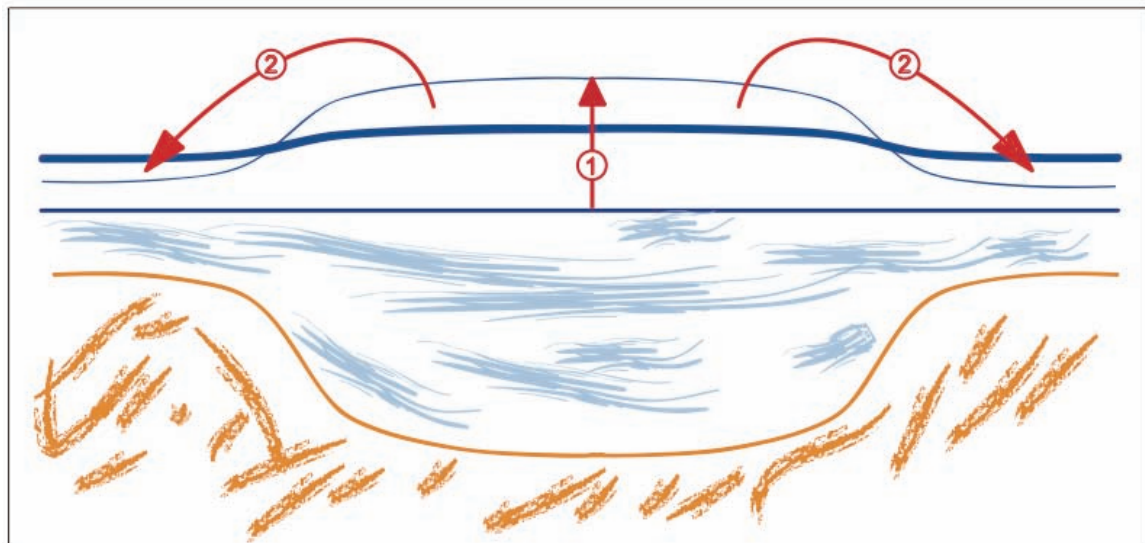


Figure 1.

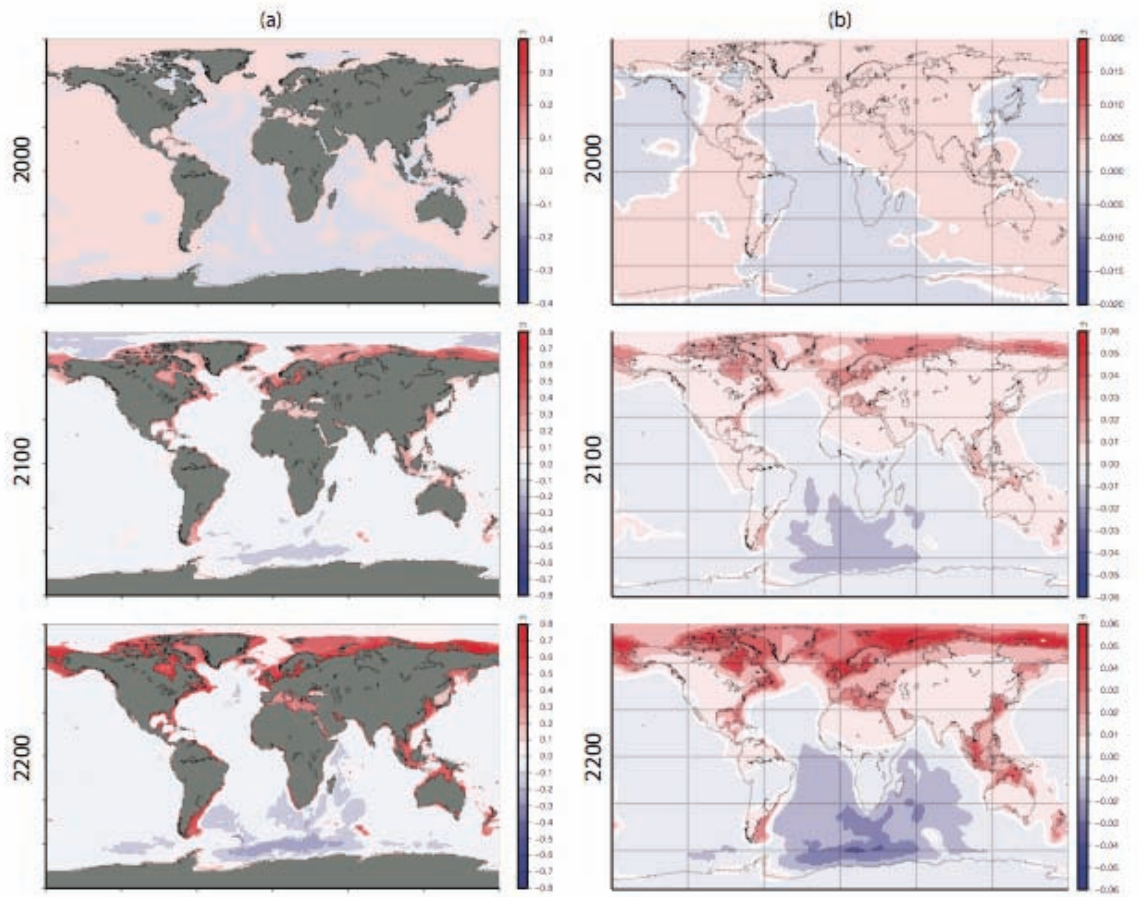


Figure 2.

The roles of bottom topography and internal gravity waves in horizontal convection

Ross W. Griffiths¹, Graham O. Hughes¹, Melissa A. Coman¹, Kial D. Stewart¹

¹ *Research School of Earth Sciences, Australian National University, Canberra, ACT 0200, Australia*

Horizontal convection is the flow generated by heating and cooling along one horizontal boundary of a box. Studies of this form of convection have yielded much insight into the fundamental dynamics governing the ocean overturning circulation. In particular, equatorial surface waters are heated and high latitude surface waters are cooled, and analogies with horizontal convection allow us to investigate the role of surface buoyancy forcing in the overturning circulation. We have examined the progress in this field in a major review article published this year (Hughes and Griffiths, 2008).

In 2008 we have built on our previous studies of horizontal convection, and work has progressed on two main fronts. Firstly, we have studied the role of bottom topography in restricting flows between ocean basins, and thus in controlling the rate of overturning circulation. Secondly, we have discovered the spontaneous generation of internal gravity waves in the convective flow.

Laboratory experiments (figure 1) have shown that the introduction of bottom topography blocks the circulation, isolating waters in adjoining basins below the level of the sill. The circulation is most strongly affected when the depth of the sill is comparable with the depth to which the surface thermal boundary layer extends (i.e. the thermocline). In this regime, the range of densities in the flow increases markedly and the rate of overturning decreases. On this basis we expect the Denmark Straits and Faroe Bank Channel in the North Atlantic and the Weddell Sea ice shelf overflow in the Southern Ocean to influence the global overturning circulation.

Numerical simulations of horizontal convection have revealed the existence of coherent propagating waves (figure 2). Further investigation has shown that highly localized sinking plumes (as in figure 1) perturb the density stratification and excite a spectrum of internal gravity waves. We have been able to identify interaction of these wave modes as a source of strong variability in the circulation. Further work is required to assess the importance of this phenomenon in the ocean overturning circulation.

Hughes, G.O. and Griffiths, R.W. (2008) Horizontal convection. *Annu. Rev. Fluid Mech.* **40**, 185–208.

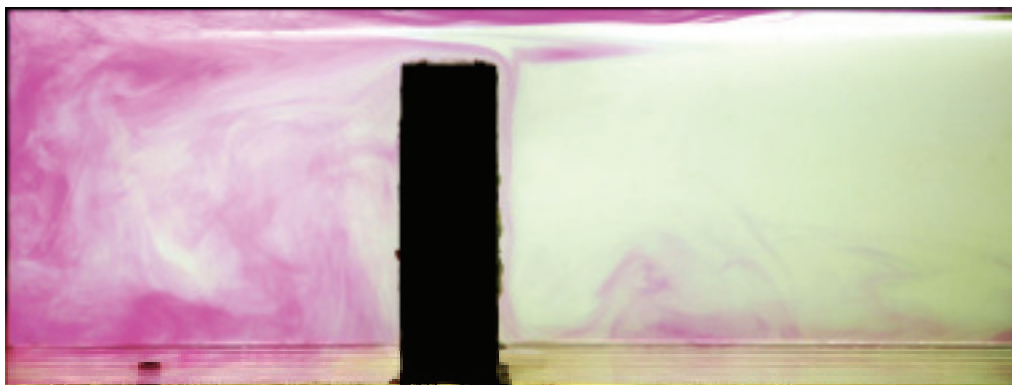
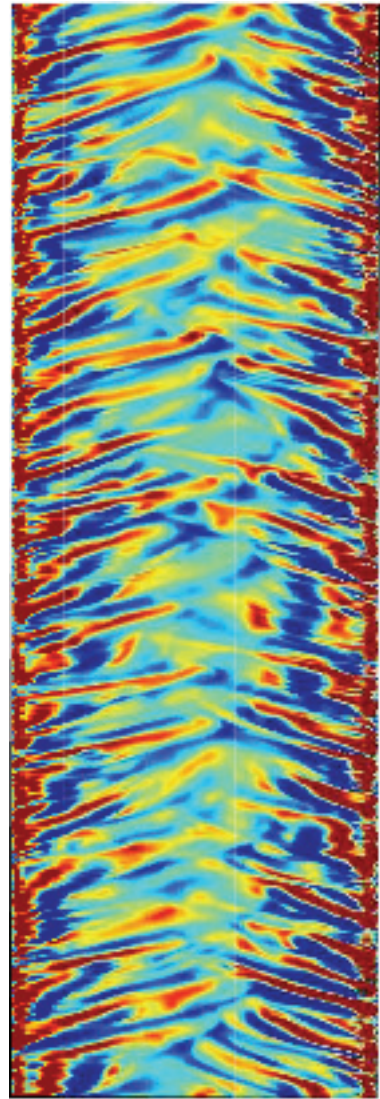


Figure 1. Dye visualization of a horizontal convection experiment with bottom topography (the field of view includes only the left-hand half of the box). The overturning circulation is forced by surface cooling at the left-hand end of the box ("polar latitudes") and surface heating over the right-hand end ("equatorial latitudes"; not visible). The dye reveals that relatively warm surface waters flow from right to left above the sill, where they subsequently become very cold, sink, and are trapped on the left of the topography at levels below the sill. This trapped water eventually fills the left-hand basin and can be seen leaking across the top of the sill (from right to left), whence it enters the main basin as a highly localized sinking plume.

Figure 2. Hovmöller plot of the vertical velocity along a horizontal section at mid-depth from a 2-D numerical simulation of horizontal convection. Time increases upwards; blue represents upwelling motion, green approximately no motion, and red downwelling motion. Regions of high latitude sinking are situated in this case at both the left and right hand ends of the horizontal section, and excite strong wave modes that propagate towards 'low latitudes' at the centre of the section. These waves and their interactions appear to be responsible for much of the variability in the circulation.



Multi arrival tomography

Juerg Hauser¹, Malcolm Sambridge¹ and Nicholas Rawlinson¹

¹ *Research School of Earth Sciences, Australian National University, Canberra, ACT 0200, Australia*

In seismic imaging the focus has largely been on first arrivals, with a wide variety of schemes developed for their calculation. However, later arrivals often contribute to the length and shape of a recorded wave train, particularly in regions of complex geology. They are likely to contain additional information about seismic structure as their two point paths, differs from that of the first arrival. If they can be used in seismic tomography, improved images should result. Here we use the wavefront construction principle as the basis of a new scheme for computing travel times for first and later arrivals that arise from smooth variations in both velocity structure and interface geometry.

To investigate the possibility of using later arrivals to improve seismic imaging a numerical test is performed. We compare the results of first and multi arrival tomography, when recovering a two layered crustal scale structure characterised by two low velocity anomalies and a u-shaped valley in the interface. The inversion is performed simultaneously for interface and velocity structure. There are sources above and below the interface and two incoming plane waves are also simulated. Figures 1.a and 2.a show the ray path coverage of the structure, which we will try to recover using travel times. Clearly the later arrivals not only contain additional information about the two low velocity anomalies but also about the shape of the valley in the interface. Figure 1.b shows the difference between the inversion result and the true structure when only first arrivals are used in the inversion. The trade off between interface geometry and velocity anomaly is clearly not as well resolved compared to when both first and later arrivals are used (figure 2.b).

This example demonstrates that multi arrival tomography has the potential to lead to an improved recovery of structure. An important difference between first and later arrivals is that the existence of a later arrival is a function of the structure. This means that during the iterative inversion procedure, the number of ray paths and hence data is not constant. Using later arrival therefore makes the inverse problem much more non-linear, which means that care must be taken to avoid instabilities in an iterative non-linear approach.

Potential applications of multi arrival tomography include surface wave tomography, where observations of multipathing has been a long recognised phenomenon, with measurements and analysis using earthquake sources dating back many decades.

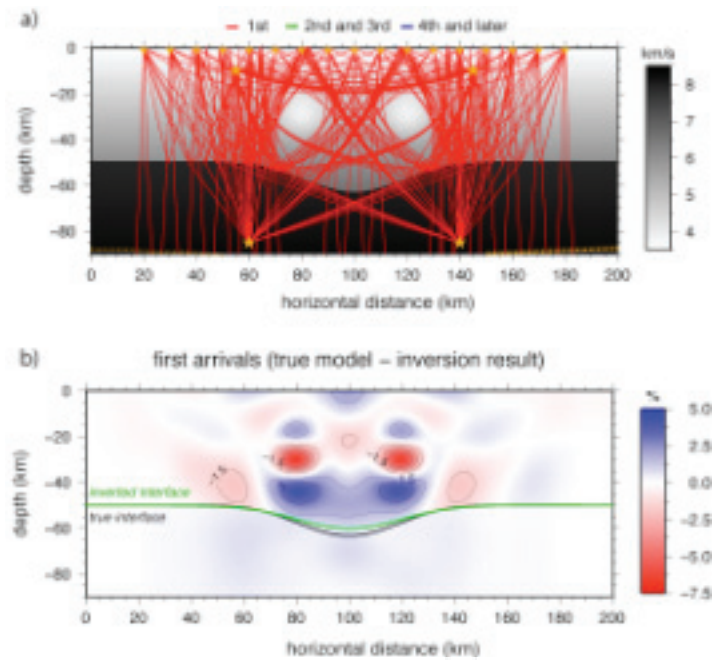


Figure 1. a) Layered velocity model and associated first arrival paths used in the inversion test. Point sources are denoted by stars and receivers by triangles. Note that paths also emanate from two impinging plane waves. b) Relative error in percent between the true model and the inversion result. Contour lines are plotted at 1.5% intervals.

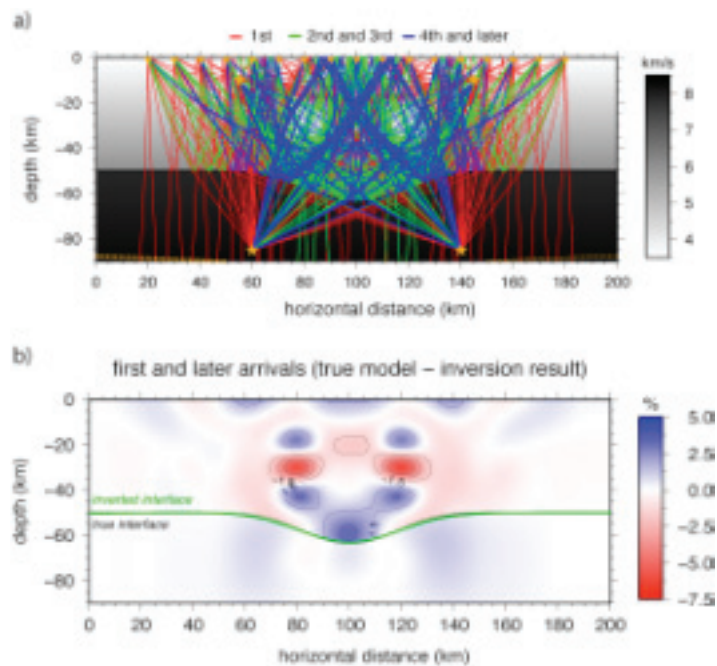


Figure 2. a) Layered velocity model and associated first and later arrival paths used in the inversion test. Point sources are denoted by stars and receivers by triangles. Note that paths also emanate from two impinging plane waves. b) Relative error in percent between the true model and the inversion result. Contour lines are plotted at 1.5% intervals.

The effects of mesoscale ocean-atmosphere coupling on the large-scale ocean circulation

Andrew McC. Hogg¹, William K. Dewar², Pavel Berloff^{3,4}, Sergey Kravtsov⁵ and David K. Hutchinson¹

¹ *Research School of Earth Sciences, Australian National University, Canberra, ACT 0200, Australia*

² *Department of Oceanography, Florida State University, Tallahassee, USA*

³ *Woods Hole Oceanographic Institution, USA*

⁴ *Cambridge University, UK*

⁵ *University of Wisconsin, Milwaukee, USA*

Recent satellite measurements of wind stress at the ocean-atmosphere interface have pointed to large variations in stress on very fine scales. These fine scales are set by ocean mesoscale dynamics, and the variations in stress occur due to coupled interaction between the ocean and atmosphere. Given that wind stress drives the ocean circulation, there is a realistic possibility for coupled feedback acting to alter ocean currents.

We model this ocean-atmosphere interaction using high-resolution ocean model, coupled to a dynamic atmospheric mixed layer. The goal is to answer the question: Do small-scale variations in stress alter the large-scale ocean circulation?

The model results show that, despite the small spatial scale of the forcing anomalies, mesoscale coupling reduces the strength of the large-scale ocean circulation by approximately 30-40%. This result is due to the highest transient wind stress curl (or Ekman pumping) anomalies (see Fig. 1) destabilising the flow in a dynamically sensitive region close to the western boundary current separation.

These results indicate the complexity involved in migrating ocean models to eddy-resolving scales. The next generation of ocean models need to resolve atmospheric boundary layer processes at the same resolution as the ocean model.

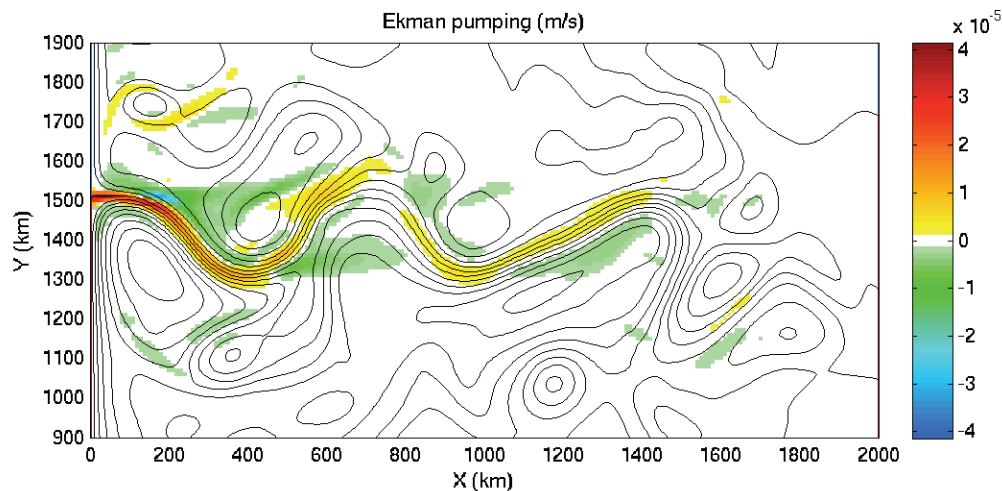


Figure 1. Snapshot of wind stress curl (or Ekman pumping) in colour, with contours of streamfunction superimposed. The streamfunction shows a western boundary current separating from the boundary, and forming a meandering zonal jet in the interior. This jet is accompanied by strong sea surface temperature gradients, which interact with the atmospheric boundary layer to produce large values of wind stress curl over the core of the jet. This extra forcing, somewhat paradoxically, acts to reduce the circulation by destabilizing the mean flow.

Energetics of the global ocean overturning circulation

Graham O. Hughes¹, Andy McC. Hogg¹, Ross W. Griffiths¹

¹ *Research School of Earth Sciences, Australian National University, Canberra, ACT 0200, Australia*

The overturning circulation of the global oceans regulates Earth's climate, and oceanographers have been interested in which energy sources maintain that circulation. Energy input from surface winds and tides is important, but whether or not surface heating and cooling also contribute has been the subject of considerable debate. An understanding of the energetics is essential in addressing problems such as the response of the overturning circulation to forcing changes and in highlighting processes that need to be addressed in the development of general circulation models and climate models.

This year we have developed a theoretical framework that can be used to study the energy budget of the ocean overturning circulation. The concept of available potential energy, which is a measure of how far the density field is from equilibrium, underpins this framework. We have demonstrated that surface buoyancy forcing generates available potential energy, and is indeed an important energy source for the overturning circulation. In particular, only mixing and surface buoyancy forcing act to change the density of waters and, in a steady circulation, the energy transports associated with these two processes must balance. We have further clarified how the sources of kinetic energy associated with the winds and tides are simultaneously necessary to maintain the observed ocean overturning circulation.

We have in conjunction with our theoretical work undertaken a series of high-resolution numerical computations using a general circulation model of an ocean basin (figure 1). The results confirm our theoretical findings. Importantly, they also show that deductions regarding the energy budget of the ocean overturning circulation are strongly influenced by parameterizations of small-scale processes that are in common use in numerical models.

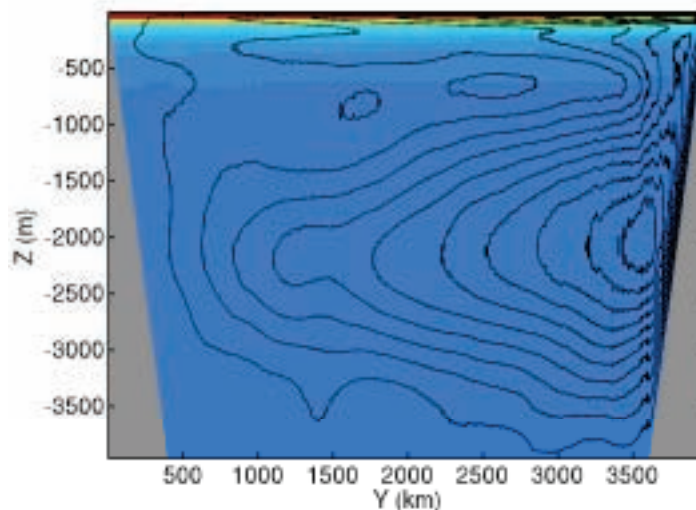


Figure 1. The time-averaged overturning circulation obtained in 2-D numerical simulations of a model ocean basin forced only by surface heating and cooling (varying smoothly from 200 W/m^2 at the left end to -200 W/m^2 at the right end, but with no net heat input to the basin). The simulation was non-hydrostatic, was conducted at high resolution (10–75 m vertical resolution and 0.75–7.5 km horizontal resolution), and was run with a vertical diffusion coefficient of $10^{-4} \text{ m}^2/\text{s}$. The coldest waters are coloured blue and warmer waters towards the surface are shown as yellows and reds. The maximum overturning streamfunction is $28 \times 10^3 \text{ kg/s}$ per unit width.

Effect of thermal diffusion on the stability of strongly tilted mantle plume tails

Ross Kerr¹, John Lister² and Catherine Mériaux³

¹ Research School of Earth Sciences, Australian National University, Canberra, ACT 0200, Australia

² Institute of Theoretical Geophysics, Department of Applied Mathematics and Theoretical Physics, University of Cambridge, Cambridge CB3 0WA, United Kingdom

³ School of Mathematical Sciences and MC², Monash University, Victoria 3800, Australia

Mantle plumes are produced by heat conducted into the Earth's mantle from the underlying core. This heating forms a thermal boundary layer of hot, low viscosity fluid, which focuses into narrow plumes that rise through the mantle. At the Earth's surface, partial melting of the plumes produces flood basalts from plume heads and volcanic island chains from plume tails.

As plume tails rise through the mantle, they are deflected by large-scale convection driven by the subduction of cold lithospheric plates. Last year, we reported a series of laboratory experiments that investigated the effect of thermal diffusion on the gravitational stability of these plume tails when they have been strongly tilted. This year, we examined this instability using a series of numerical calculations (Figure 1).

At large viscosity ratios, we conclude that the instability is unaffected by thermal diffusion when the Rayleigh number Ra is greater than about 300. When Ra is less than 300, thermal diffusion significantly increases the time for instability, as the rising fluid region needs to grow substantially by entrainment before it becomes unstable. When Ra is less than about 140, and the rise height available is less than about 40 times the cylinder radius, the rising region of fluid is unable to grow sufficiently and instability is prevented. When our results are applied to the Earth, we predict that thermal diffusion will stabilize plume tails in both the upper and lower mantle (Kerr, Mériaux and Lister 2008). We also predict that some of the buoyancy flux in mantle plumes is lost during ascent to form downstream thermal wakes in any larger scale mantle flow.

Kerr RC, Mériaux C, Lister JR (2008) Effect of thermal diffusion on the stability of strongly tilted mantle plume tails. *Journal of Geophysical Research* 113: B09401, doi:10.1029/2007JB005510

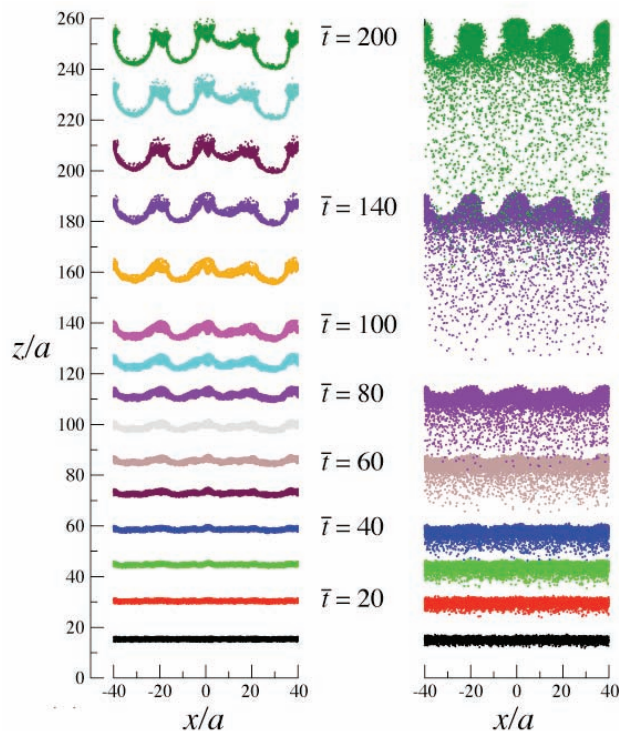


Figure 1. Numerical calculations showing the rise and eventual instability of a cylinder of buoyant fluid, as a function of dimensionless time. The cylinder has an initial radius a , and a Rayleigh number of 80. The side views show the distribution of tracers (left) and buoyancy (right).

Testing the Plume Hypothesis: Laboratory models of Subduction-plume interaction for the Cascades and Tonga-Lau Convergent Margins

Chris Kincaid¹, Ross Griffiths², the High Lava Plains Working Group³ and the Somoan Plume working group⁴.

¹ *Graduate School of Oceanography, University of Rhode Island, Narragansett, RI, USA*

² *Research School of Earth Sciences, Australian National University, Canberra, ACT 0200, Australia*

³ *Richard Carlson & David James (Carnegie Inst. Of Wash.), Tim Grove (MIT), William Hart (Miami Univ.), Anita Grunder & Robert Duncan (Oregon State Univ.), Matt Fouch (Ariz. State Univ.), Randy Keller (Univ. of Oklahoma), Steve Harder (Univ. of Texas), Maureen Long (Yale Univ.).*

⁴ *Stan Hart, Mark Behn & John Collins (Woods Hole), Greg Hirth (Brown Univ.), Magali Billen (Univ. of California, Davis).*

Subduction of lithospheric plates back into the mantle at subduction zones (ocean trenches) provides the dominant driving force for plate tectonics and causes thermal and chemical exchange with the Earth's interior. We have developed a laboratory apparatus for modeling 3D aspects of flow in subduction zones in response to various modes by which plates move and subduct into the mantle. These include slab rollback, when the slab sinks with a backward retreating or horizontal component of motion, and periods where the angle of descent (slab dip) either increases or decreases with time. Previous work has documented the importance of these modes of plate motion on 3D shallow mantle return flow and both slab and mantle wedge temperatures (Kincaid and Griffiths, 2003; 2004).

Kincaid and Griffiths are involved with two NSF funded projects to look at aspects of plume vs. non-plume models for reconciling patterns in geophysical and geochemical data collected within subduction zones. One project (the High Lava Plains project) involves a combination of efforts (seismology, geology/geochemistry and geodynamics) to better understand the evolution of the Cascades subduction system, spatial-temporal patterns in melt production and continental growth in the northwestern USA. In addition to field geology, this effort involves an a spatially detailed broadband seismic experiment coupled with a recent large scale active source seismic experiment. In terms on modeling, Kincaid and Griffiths are exploring aspects of 3D mantle flow and both thermal and compositional evolution of the mantle, and spatial-temporal patterns melt production for a subduction zone with representative plate motions for the Cascades-Pacific northwest USA system.

Plume-subduction interaction experiments show that plumes can be strongly deformed by rollback subduction and can be efficiently drawn into the arc wedge corner over large horizontal distances (~1000 km). The combination of rollback subduction and backarc extension deform the plume head and tail in a way that produces an early, circular large volume melt feature and two subsequent linear melt production features which are offset in space and time (~15 Ma). Two tracks are formed with time-transgressive rhyolite melting (e.g. reheating of the plate) and basaltic melt production, which trend in opposite directions. One is similar to the High Lava Plains in central Oregon, and the other is similar to the Snake River Plain. The initial, circular magma production feature is offset from the linear features by 300-400 km in a trench-parallel direction. The style of back-arc spreading changes the offsets and orientations of these three basic features. The influence of plate steepening is to deform the plume material into a very narrow feature. The severe, rapid deformation of plume material works to limit rise rates, essentially trapping much of this material deep in the wedge. The combined effects of increased diffusion and small length scales, partial melting and severe distortion in 3D, will make these remnant plume features difficult to image with seismic techniques.

In 2008 a URI PhD student, Ms Kelsey Druken, is working to extend these models of Cascades subduction system, including the effect of a keel-like morphology (Figure 1a) for the base of the overriding plate. An important part of the project is to also test

non-plume models. Three-dimensional flow-fields (Figure 1) are being analysed in combination with temperature data and a melt production model to calculate spatial patterns in vertical heat and melt flux through time for non-plume cases. In addition, finite strain is being observed within the flow through the use of whiskers. These act as a proxy for olivine alignment within the upper mantle and are being compared with seismic anisotropy data collected from the High Lava Plains.

Kincaid, C., and R. W. Griffiths (2003) Thermal evolution of the mantle during rollback subduction, *Nature*, 425, 58-62

Kincaid, C. and R. W. Griffiths (2004) Variability in mantle flow and temperatures within subduction zones. *Geochem. Geophys. Geosyst.*, 5, Q06002, doi:10.1029/2003GC000666

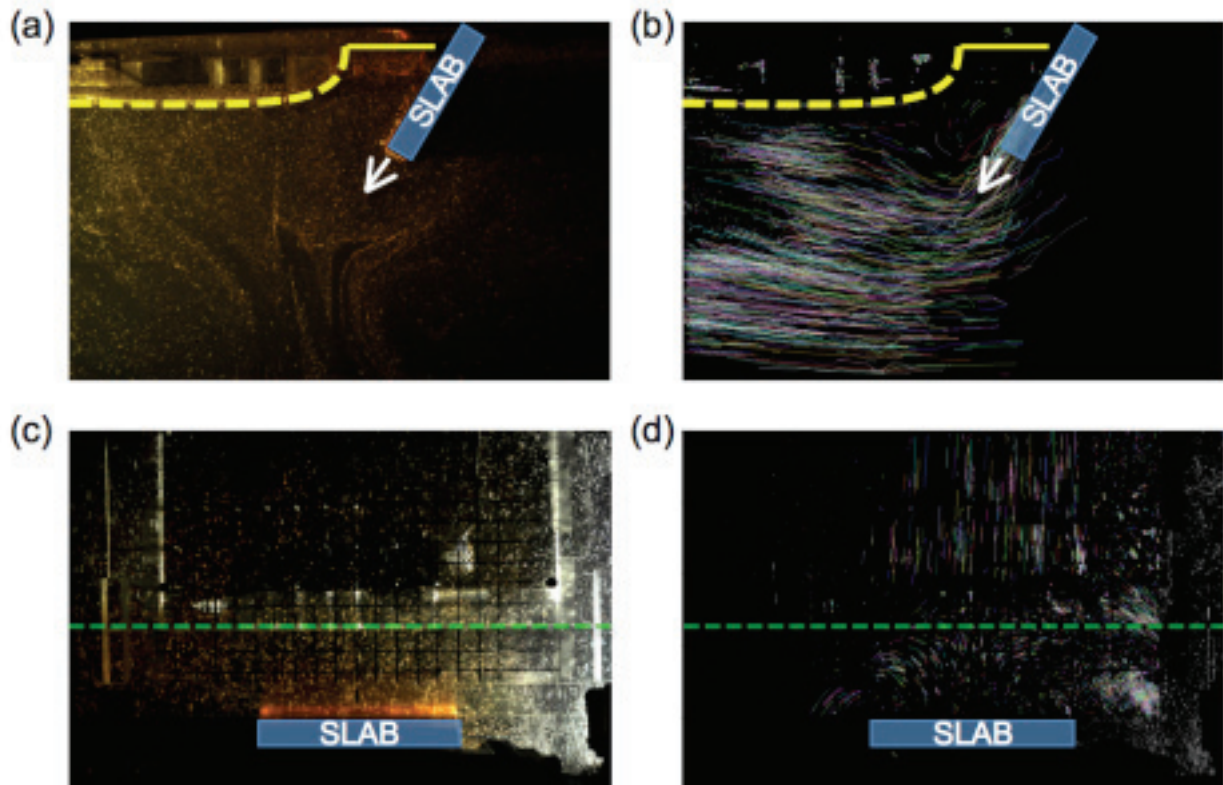


Figure 1: Top- and side-view images of the non-plume modelling of the Cascades using the 3D subduction system. that includes down-dip slab motion (5 cm/Ma), rollback slab motion (2.8 cm/Ma) and westward drift of the overriding plate (OP) at 1.4 cm/Ma. The combination of trench rollback and OP westward motion give a net extension rate about the spreading center (green dashed line) of 1.4 cm/Ma. Vertical and horizontal slices are imaged to produce 3D flow fields using particle tracking velocimetry (PTV) in FluidStream (developed by R. Nokes) (a) Side-view slice 4.5 cm (225 km scaled) along trench from plate centerline illustrating the subducting slab and the keel-like morphology of the over-riding plate (dashed yellow line) (b) Path-lines from PTV on the side-view slice using FluidStream. (c) Top-view slice at 2 cm (100 km scaled) depth where the back-arc spreading center (green dashed line) marks the start of the thickened morphology of the over-riding plate. (d) Path-lines for the top-view image using FluidStream PTV analysis.

Seismic Investigations of Lithospheric Transitions between the Northern and Southern Australian Cratons (BILBY)

Sara H. Pozgay¹ and Brian L.N. Kennett¹

¹ *Research School of Earth Sciences, Australian National University, Canberra, ACT 0200, Australia*

We aim to determine the nature of the transition at lithospheric depths between the northern and southern Australian cratons. What are the controlling factors of the regions with anomalously slow velocities beneath the central Australian intercratonic suture zones? Do these intercratonic transitions propagate with depth and, if so, in what manner? To answer these questions, 25 broadband seismic stations were deployed in August–September 2008 and will remain operational for approximately one year.

Much of the Australian continent is an amalgamation of several smaller cratons and multiple orogenic events. The transitions between any two cratonic regions, however, do not necessarily reflect the same processes. Beneath the Capricorn Orogen (connecting the Yilgarn and Pilbara cratons), seismically fast wavespeeds (relative to a reference earth velocity model) and low attenuation are relatively continuous from 75 to >300 km depth. These large-scale observations suggest that a simple thermal origin is a likely explanation for the seismic signature of the orogen. However, much of central Australia is different; the central intercratonic belt regions exhibit low attenuation as for the case of the Capricorn Orogen, but slow wavespeeds persist at ~75 km depth. Only 25 km deeper, wavespeeds are fast and become relatively continuous at ~125 km depth. These observations suggest that the physical mechanism responsible for the observed seismic signature is more complex than simple thermal variations would predict.

What is the nature of this slow wavespeed region around 75 km depth beneath these intercratonic suture belts? Do the transitions between them extend through the whole lithosphere, as suggested by prior studies of the central Australian (Arunta Block) region? Several orogenic events should have made a lasting imprint through the whole lithosphere (e.g. the Alice Springs Orogeny 400–300 Ma), however these effects have yet to be imaged at the appropriate resolution to determine the nature of different lithospheric sections. Prior seismic deployments in the region were largely designed to image either crustal fault systems or deep lithosphere and upper mantle structures and, therefore, can provide only first-order constraints on the intercratonic suture belts.

We deploy an ambitious seismograph station configuration to image these lithospheric transitions between the northern and southern Australian cratonic regions and across parts of the intercratonic suture belts. The experiment configuration is designed specifically to connect the Gawler Craton in the south to components of the North Australian Craton – specifically, through the Musgrave Block and to the northern side of the Arunta Block, and to connect the Arunta Block with the Mt. Isa Block. A combination of rigorous analysis tools, such as velocity and attenuation tomography coupled with receiver functions, will help to provide a comprehensive understanding of the amalgamation of continental cratons and the associated intercratonic transitions. In addition, a significant amount of information will be added to the present understanding of intercratonic suture belts and further constraints on the Australian lithospheric structure and overall continental amalgamation will be realised.

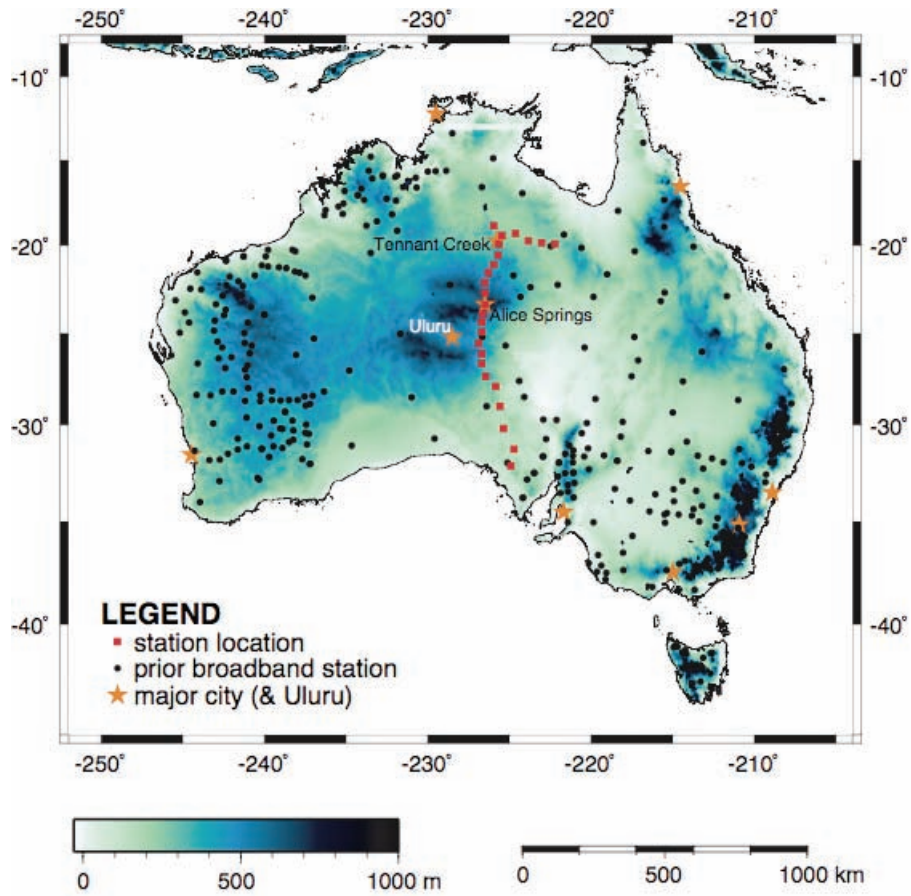


Figure 1. BILBY station map. Red squares indicated proposed station locations; black circles are prior broadband instrumentation; orange stars are major landmarks. Topography scale (in meters) shown at bottom.



Figure 2. Station near Alice Springs.

Exploring deep Australia with the WOMBAT array

Nick Rawlinson, Brian Kennett and Hrvoje Tkalčić

Research School of Earth Sciences, Australian National University, Canberra, ACT 0200, Australia

In the last decade, a dense rolling array of short period seismometers has been used to achieve a cumulative coverage of over 400 sites throughout southeast Australia (see Figure 1). This experiment, known as WOMBAT-SE, has recorded large volumes of passive seismic data for use in teleseismic tomography, ambient noise tomography, receiver function analysis and array studies of deep mantle and core structure. Station spacings vary between approximately 15-20 km in Tasmania, and 30-50 km on mainland Australia. Deployment times of early experiments in western Victoria and southeast South Australia are approximately 4 months, but since EVA (Figure 1), they have been extended to 8-12 months. The majority of instruments used have been ANU solid state short period recorders connected to vertical component L4Cs (natural frequency of 1Hz), but since SETA (Figure 1), three-component Lennartz LE-3Dlite sensors (also with a natural frequency of 1Hz) have been deployed.

To date, a variety of studies have been carried out with the recorded data, including teleseismic tomography, joint inversion of passive and active source data, ambient noise tomography, and analyses of exotic core phases. In this report, early results from a combined inversion of teleseismic arrival time residuals will be featured. Figure 2 shows a tomographic image at 150 km depth produced by the inversion of EVA, LF98, MB99, SEAL and SEAL2 datasets. One of the clearest features in Figure 2 is the east to west change from slower to faster velocities from the Bendigo Zone to the Stawell Zone. It is tempting to interpret this as a change from Phanerozoic mantle lithosphere of oceanic origin to Proterozoic mantle lithosphere of continental origin. Expected changes in both composition and temperature between these two types of material make this a plausible argument. In addition, this approximate boundary has also been observed, albeit at lower resolution, using surface-wave tomography, which appears to clearly distinguish between cratonic western Australia and the younger orogens that characterise eastern Australia. However, it must be remembered that recent overprinting effects, such as the hotspot-related Newer Volcanic Province in Victoria and magmatic processes related to the opening of the Bass and Otway basins and the Tasman Sea, may well have contributed significantly (via increased temperatures) to reduced wavespeeds observed in central and southern Victoria.

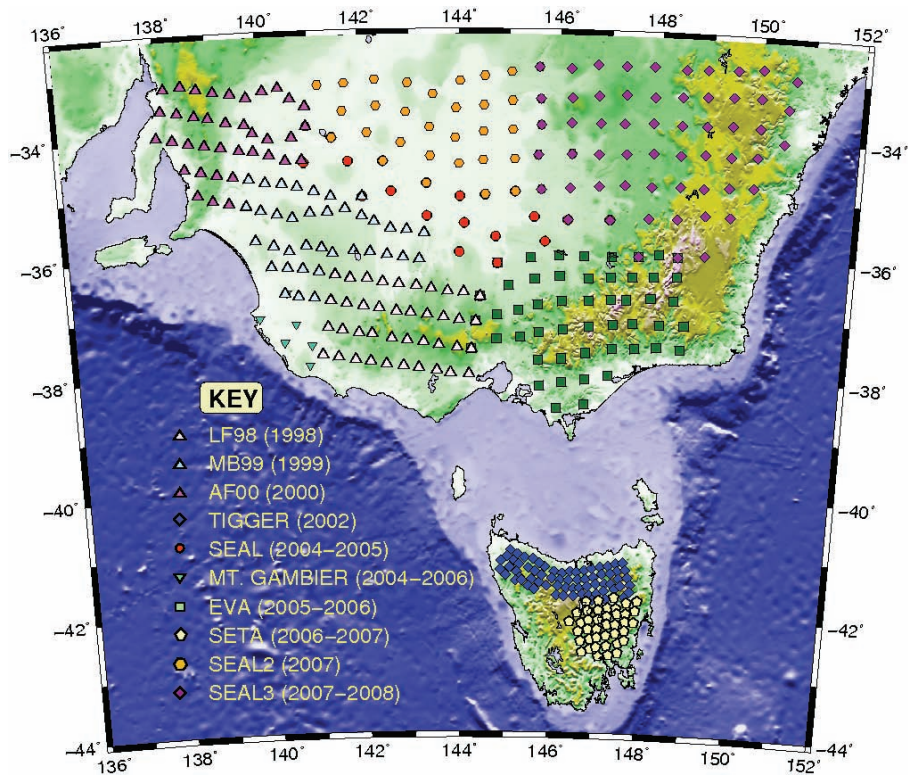


Figure 1. Location of all short period passive seismic arrays deployed in southeast Australia over the last decade

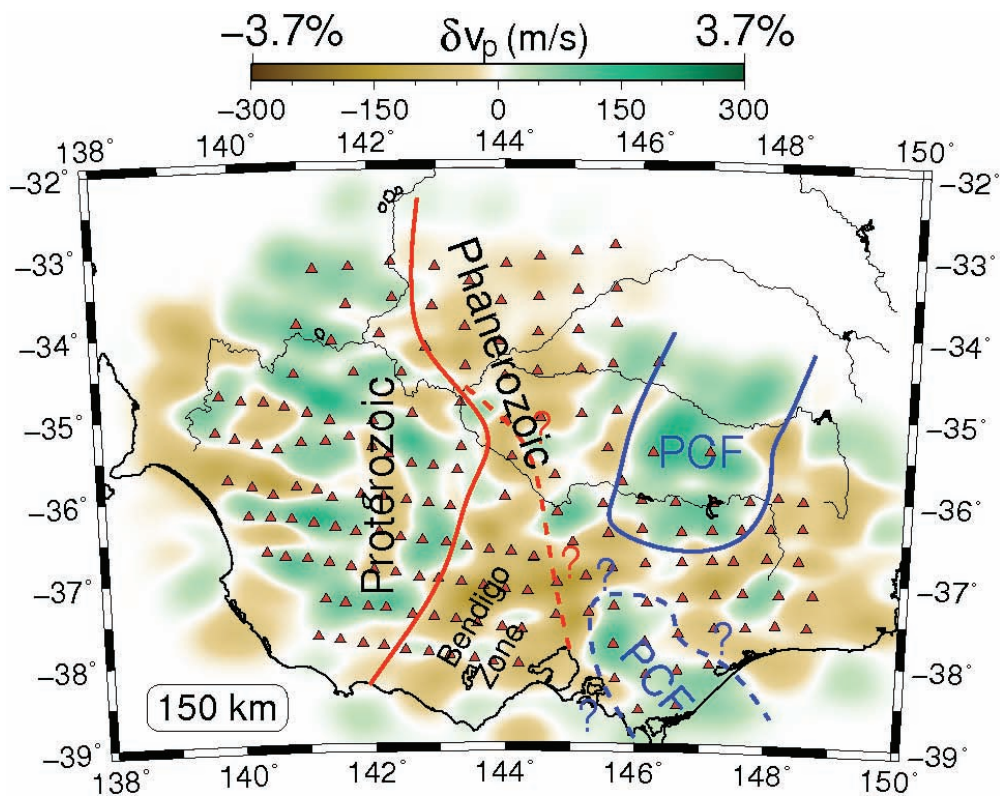


Figure 2: Preliminary image obtained from joint inversion of teleseismic arrival time residuals recorded at five arrays of the WOMBAT-SE project. PCF = Proterozoic Continental Fragment.

The dynamics of solidifying lava flows with a Bingham yield strength rheology

Jesse Robertson¹, Ross Kerr¹ and Ross Griffiths¹

¹ *Research School of Earth Sciences, Australian National University, Canberra, ACT 0200, Australia*

Lava flows cover much of the Earth, the Moon, Mars, Venus, and several satellites of the outer planets. They vary greatly in their viscosities and eruption rates and form a wide range of flow types from long channel and tube flows to lava domes. Recent research in the GFD Laboratory has focused on surface crust formation, channel formation and flow morphology in Newtonian fluids subject to surface cooling (Griffiths et al. 2003; Kerr et al. 2006). This work predicts the behaviour of crystal-poor lava flows with a Newtonian rheology, such as some proximal basaltic flows on Kilauea Volcano, Hawaii and submarine lava flows near submarine spreading ridges. However, many lava flows contain sufficient crystals for the lava to have a viscoplastic rheology with a substantial yield strength, including those typical of distal Hawaiian channels and most Mt Etna flows. The yield strength can have a significant effect on the velocity distribution in a channel flow, and hence should have a major impact on the very complex interaction between convection and surface solidification seen in solidifying channel flows.

Experiments carried out this year have aimed to develop a quantitative understanding of solidification, cooling mechanisms, and tube formation in lava flows with a Bingham viscoplastic rheology. In these experiments, slurries of polyethylene glycol and kaolin flowed down a long sloping channel under water. We systematically varied flow rate, slope and channel width for flows with no cooling, flows with cooling but no solidification, and flows with cooling and solidification (Figure 1). This data set will allow us to determine the roles of yield strength, flow rate, cooling rate, slope and aspect ratio in governing surface crust distribution, the critical conditions for transition from open channel to lava tube flow, and the thermal efficiency of the flows.

Griffiths RW, Kerr RC, Cashman KV (2003) Patterns of solidification in channel flows with surface cooling. *Journal of Fluid Mechanics* 496: 33-62
Kerr RC, Griffiths RW, Cashman, KV (2006) The formation of channelized lava flows on a slope. *Journal of Geophysical Research* 111: B10206, doi:10.1029/2005JB004225

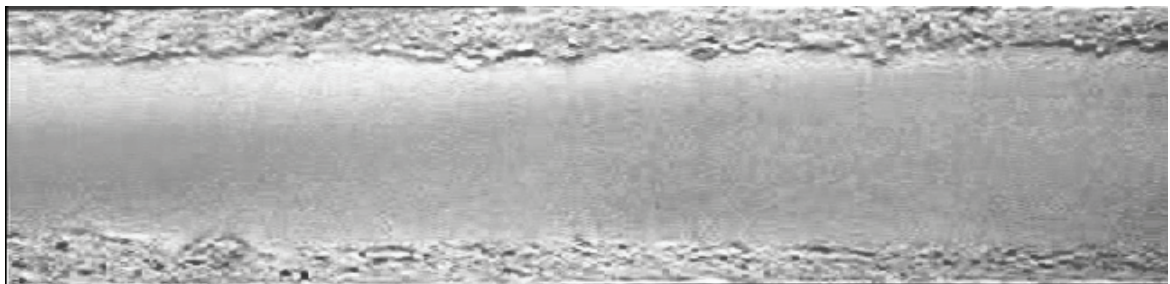


Figure 1. Overhead photograph of a slurry of polyethylene glycol and kaolin, flowing from right to left down a 8 cm wide sloping rectangular channel. The flow is overlain by cold water, and freezes to form a central raft of smooth solidified crust, separated from the walls by two shear layers.

Gawler Craton Array

Michelle Salmon¹, Brian Kennett¹

¹ *Research School of Earth Sciences, Australian National University, Canberra, ACT 0200, Australia*

As part of a wider AUSCOPE project 35 short-period seismometers have been deployed across the Gawler Craton in South Australia. Station spacing is approximately 50 km and the area covered runs from Port Lincoln in the Eyre Peninsular to Leigh Creek just west of the Flinders Ranges (figure 1.). Stations will record continuous three component data for a period of 8 months. The primary aim of this array is to increase data coverage in this part of Australia for seismic imaging. There are only two permanent seismographs in the region covered by this array. Data from this array will eventually be publicly available providing the information required to build basic images of the earth structure in the region.

The instruments are capable of recording data from both local and distant earthquakes. This area of South Australia is seismically active and local earthquake data recorded on this array (figure 2.) will help improve our ability to locate and characterize these events. Distant earthquakes will be used to produce tomographic images of the crust and upper mantle in the region. Receiver functions constructed from the three component data can will also be used to locate seismic discontinuities such as the crust-mantle boundary.

The eastern edge of the Gawler craton is currently of particular interest for the supply of geothermal energy and there are many ongoing industry projects in the area. Geoscience Australia completed a deep seismic reflection transect across the top of the Eyre Peninsular just prior to the deployment of the Gawler array. This array will provide broad scale earth imaging required for more detailed studies.

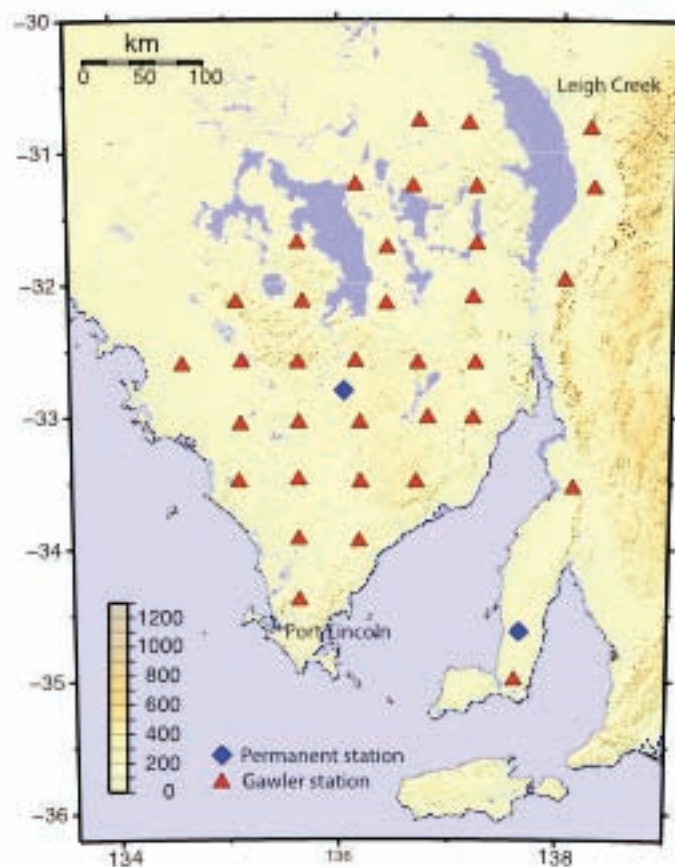


Figure 1.

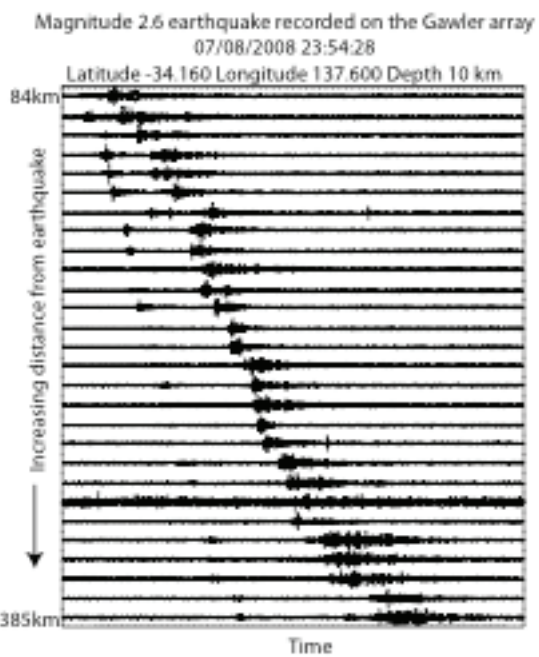


Figure 2.

Dynamic objective functions in seismic tomography

N. Rawlinson¹, M. Sambridge¹ and E. Saygin²

¹Research School of Earth Sciences, Australian National University, Canberra, ACT 0200, Australia

²Geoscience Australia, Symonston ACT 2609, Australia

A new technique designed for generating multiple solutions to seismic tomography problems using gradient based inversion has been developed. The basic principle is to exploit information gained from previous solutions to help drive the search for new models. This is achieved by adding a feedback or evolution term to the objective function that creates a local maximum at each point in parameter space occupied by the previously computed models (Figure 1). The advantage of this approach is that it only needs to produce a relatively small ensemble of solutions, since each model will substantially differ from all others to the extent permitted by the data. Common features present across the ensemble are therefore likely to be well constrained.

A synthetic test using surface wave traveltimes and a highly irregular distribution of sources and receivers shows that a range of different velocity models are produced by the new technique. These models tend to be similar in regions of good path coverage, but can differ substantially elsewhere. A simple measure of the variation across the solution ensemble, given by one standard deviation of the velocity at each point, accurately reflects the robustness of the average solution model. Comparison with a standard bootstrap inversion method unequivocally shows that the new approach is superior in the presence of inhomogeneous data coverage that gives rise to under or mixed-determined inverse problems. Estimates of posterior covariance from linear theory correlate more closely with the dynamic objective function results, but require accurate knowledge of *a priori* model uncertainty.

Application of the new method to traveltimes derived from long term cross-correlations of ambient noise contained in passive seismic data recorded in the Australian region demonstrates its effectiveness in practice, with results well corroborated by prior information (Figure 2). The dynamic objective function scheme has several drawbacks, including a somewhat arbitrary choice for the shape of the evolution term, and no guarantee of a thorough exploration of parameter space. On the other hand, it is tolerant of non-linearity in the inverse problem, is relatively straightforward to implement, and appears to work well in practice. For many applications, it may be a useful addition to the suite of synthetic resolution tests that are commonly used.

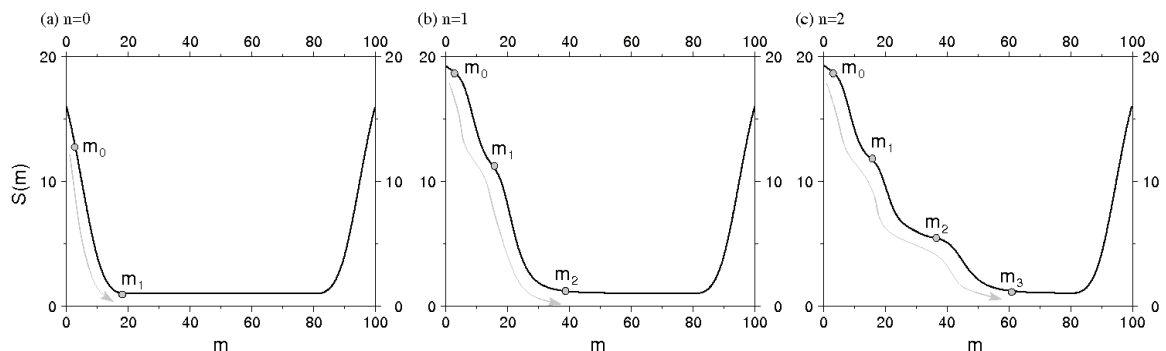


Figure 1: Schematic diagram demonstrating the principle of the dynamic objective function method. When each new solution is located by the gradient based method, a "hump" is introduced in model space at that point to dissuade future solutions from investigating this region.

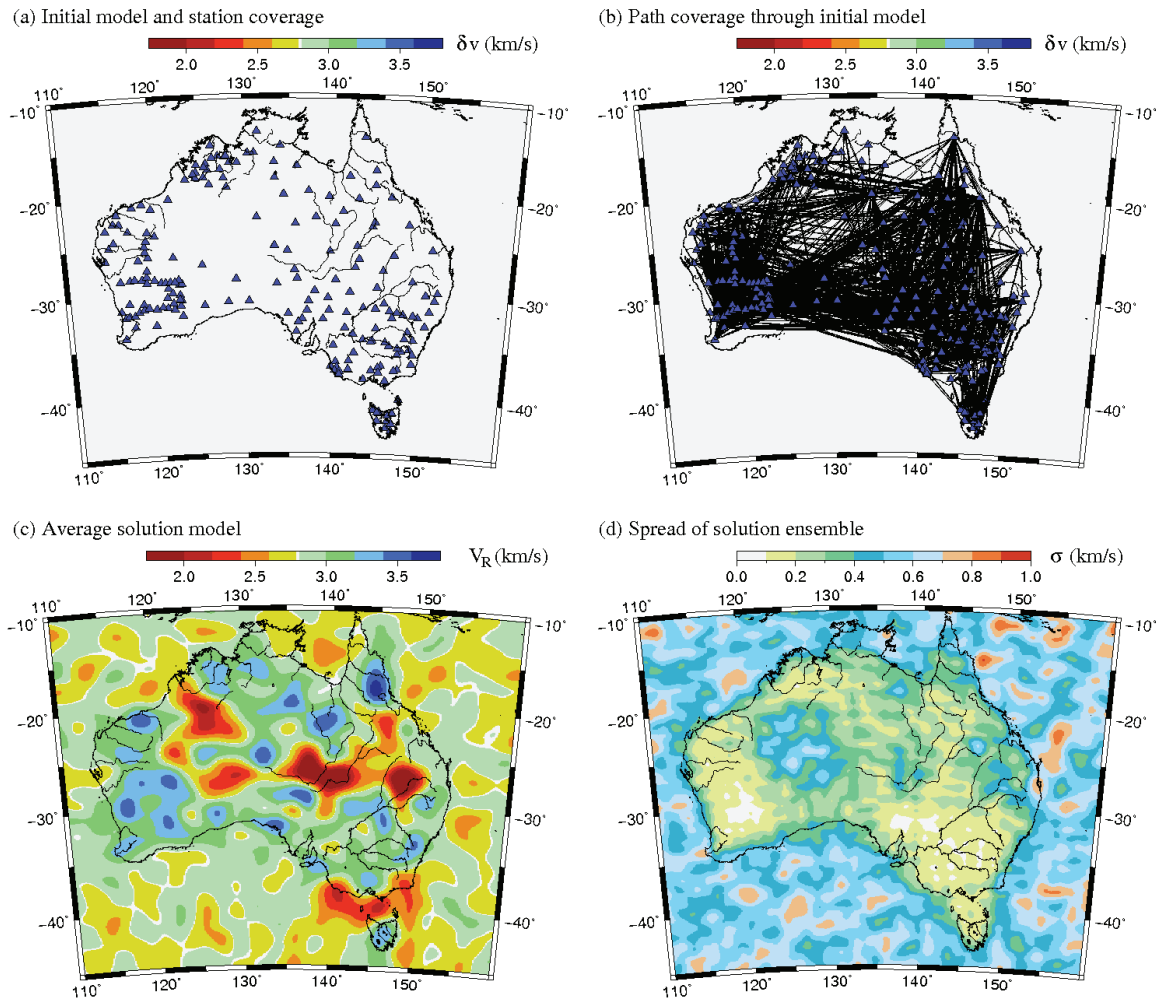


Figure 2: (a) Stations used in the cross-correlation of ambient noise data; (b) path coverage through the initial model; (c) average solution model computed from an ensemble of 25. V_R denotes Rayleigh wave group velocity; (d) variation of the model ensemble as represented by one standard deviation of the distribution.

On The Inner-Outer Core Density Contrast From New PKiKP/PcP Amplitude Ratios And Uncertainties Caused By Seismic Noise

Hrvoje Tkalčić¹, Brian L. N. Kennett¹ and V. F. Cormier²

1 Research School of Earth Sciences, Australian National University, Canberra, ACT 0200, Australia

2 Department of Physics, University of Connecticut, Storrs, 06269 – 3046 United States

The inner core boundary of the earth is characterised by a discontinuous change in elastic properties between the liquid outer and solid inner core. In the ray theory approximation, a measure of the density contrast at the inner core boundary is given by the amplitude ratio of P waves reflected from the core-mantle boundary (PcP waves) and the inner core boundary (PKiKP waves), since that ratio conveniently appears in an explicit form in the transmission/reflection coefficient equations. The results for inner-outer core density contrast derived from direct amplitude picks of these waves in the time domain have varied significantly among different authors.

The transmission/reflection coefficients on the liquid-solid and solid-liquid boundaries derived from ground displacements enable a direct comparison between the amplitude measurements on displacement seismograms in the time domain and theoretical values. A new approach is proposed and applied to integrate effects of microseismic and signal-generated noise with the amplitude measurements, thus providing a direct maximal uncertainty measure. To suppress the effects of varying radiation pattern and distinctively different ray-paths at longer epicentral distances, this new method was applied to high-quality arrivals of PcP and PKiKP waves from a nuclear explosion observed at epicentral distances 10° to 20° from recording stations. The resulting uncertainties are high precluding precise estimates of the inner core boundary density contrast, but provide a robust estimate of an upper bound from body waves of about 1100 kg/m^3 .

Median values of two amplitude ratios observed around 17° epicentral distance indicate a small density contrast of $200\text{-}300 \text{ kg/m}^3$ and suggest the existence of zones of suppressed density contrast between the inner and the outer core, a density contrast stronger than 5000 kg/m^3 at the core-mantle boundary, or a combination of both (Figure 1). Such a small estimate of the density contrast across the inner-core boundary from body waves could still produce the desired effect on the compressional velocity profile in the thermo-chemical boundary layer at the bottom of the outer core and return a modest heat flux from the inner core with a substantial inner core age, but only if accompanied by a small estimate of the density contrast of about 400 kg/m^3 from normal modes. If the inner-core boundary is characterized with such a mosaic of variable density contrast to which seismic body waves are sensitive, it is more likely that the density fluctuations are restrained to the top of the inner core. It has been argued that at least the top of the inner core is a dendritic mushy zone, in which interdendritic fluid pockets likely coexist to explain the observed nature of attenuation and attenuation in anisotropy of body waves. If PKiKP waves reflect from the inner core at the places where less dense features at the top of the inner core reduce the density contrast, than this could explain the observed lower values for stations at around 17° (Figure 1).

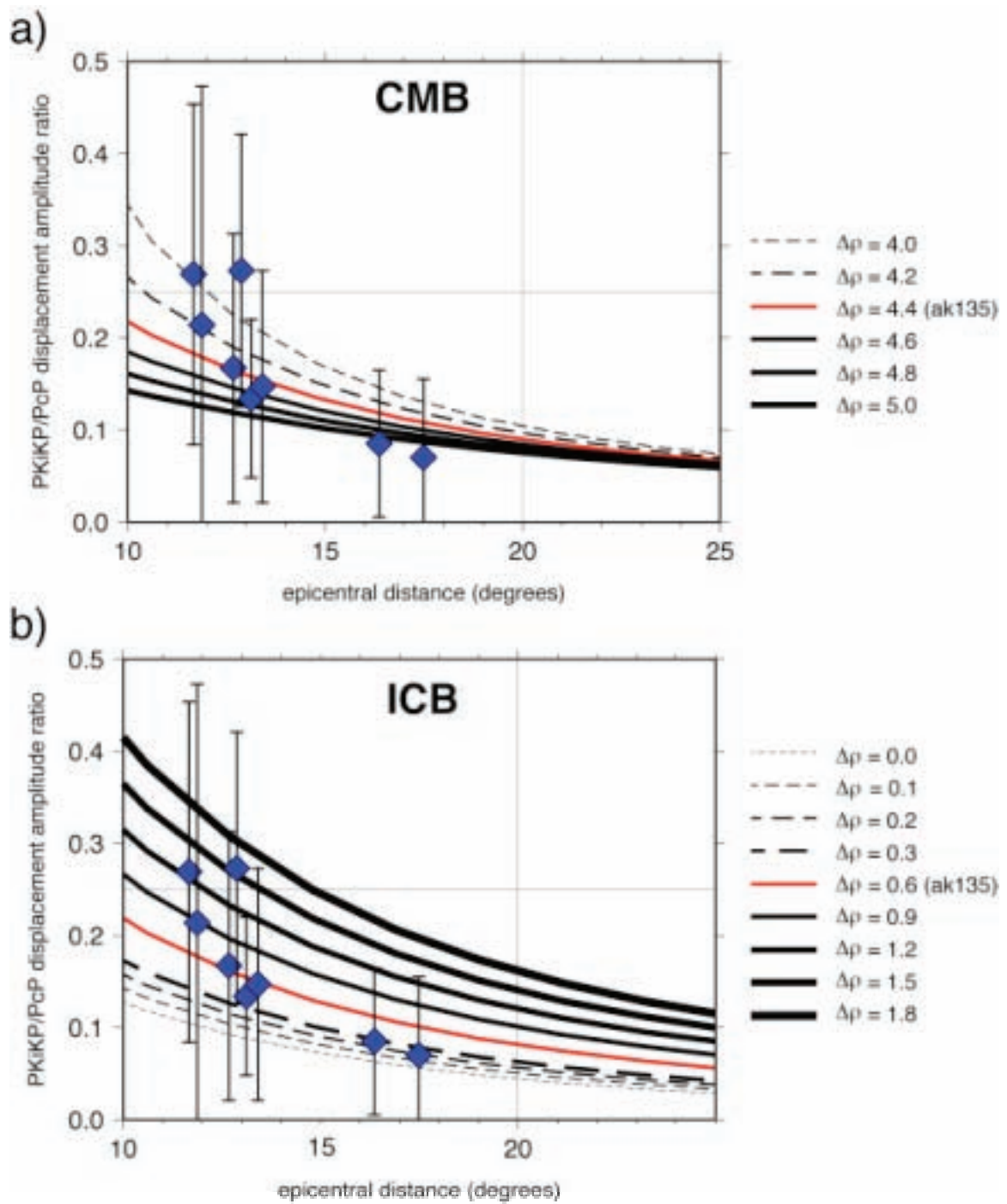


Figure 1. PKiKP/PcP amplitude measurements and their uncertainties (the median values are shown by diamonds, and the uncertainties are shown by error bars) plotted as a function of epicentral distance for: a varying density contrast at the inner core boundary (top) and the core mantle boundary (bottom). Theoretical values are indicated with lines of various thicknesses. Red line indicates the theoretical ratio from the ak135 model.

Drought in the Murray–Darling Basin

Paul Tregoning¹, Marc Leblanc² and Guillaume Ramillien³

¹ *Research School of Earth Sciences, Australian National University, Canberra, ACT 0200, Australia*

² *School of Earth and Environmental Sciences, James Cook University, Cairns, Australia.*

³ *Groupe de Recherche en Géodesie Spatiale, CNRS, Toulouse, France.*

The Murray–Darling Basin (MDB) is experiencing one of the most severe droughts in recorded history, driven by record high temperatures and several years of rainfall deficit. The multi-year drought has seen an almost complete drying of surface water resources, water that is required for agriculture and domestic use.

It has always been difficult to quantify total water storage in drainage basins because of the difficulty of measuring and monitoring water retained as soil moisture and in groundwater reservoirs. With the launch of the Gravity Recovery and Climate Experiment (GRACE) space gravity mission in 2002, it is now possible to estimate basin-scale total water storage. GRACE detects changes in the Earth's gravity field – more precisely, changes in potential between the centre of the Earth and the satellites. Making the assumption that the changes in potential are due entirely to changes in water volume, it then becomes possible to estimate the spatial and temporal variations in water integrated across large regions.

Figure 1 shows the time series of changes in total water storage of the MDB since the beginning of the GRACE mission (*Leblanc et al., 2008*) compared to groundwater, soil moisture and surface water variations. A significant loss of ~260 GTonnes of water can be seen between 2005 and 2007 in the GRACE estimates and the overall loss of total water storage correlates with groundwater losses. The meteorological drought (ie rainfall quantities) abated in 2007 and early 2008 with a return to average or above-average rainfall in the northern part of the basin. The drought actually began some years earlier; hence it is not possible to quantify the total loss of water caused by the current drought. Nonetheless, the GRACE total water storage data indicates that a substantial water deficit remains. Rainfall levels have declined below average values since March 2008.

Leblanc, M., P. Tregoning, G. Ramillien, S. Tweed and A. Fakes, Basin scale, integrated observations of the 21st Century multi-year drought in southeast Australia, *Water Resour. Res.* in revision.

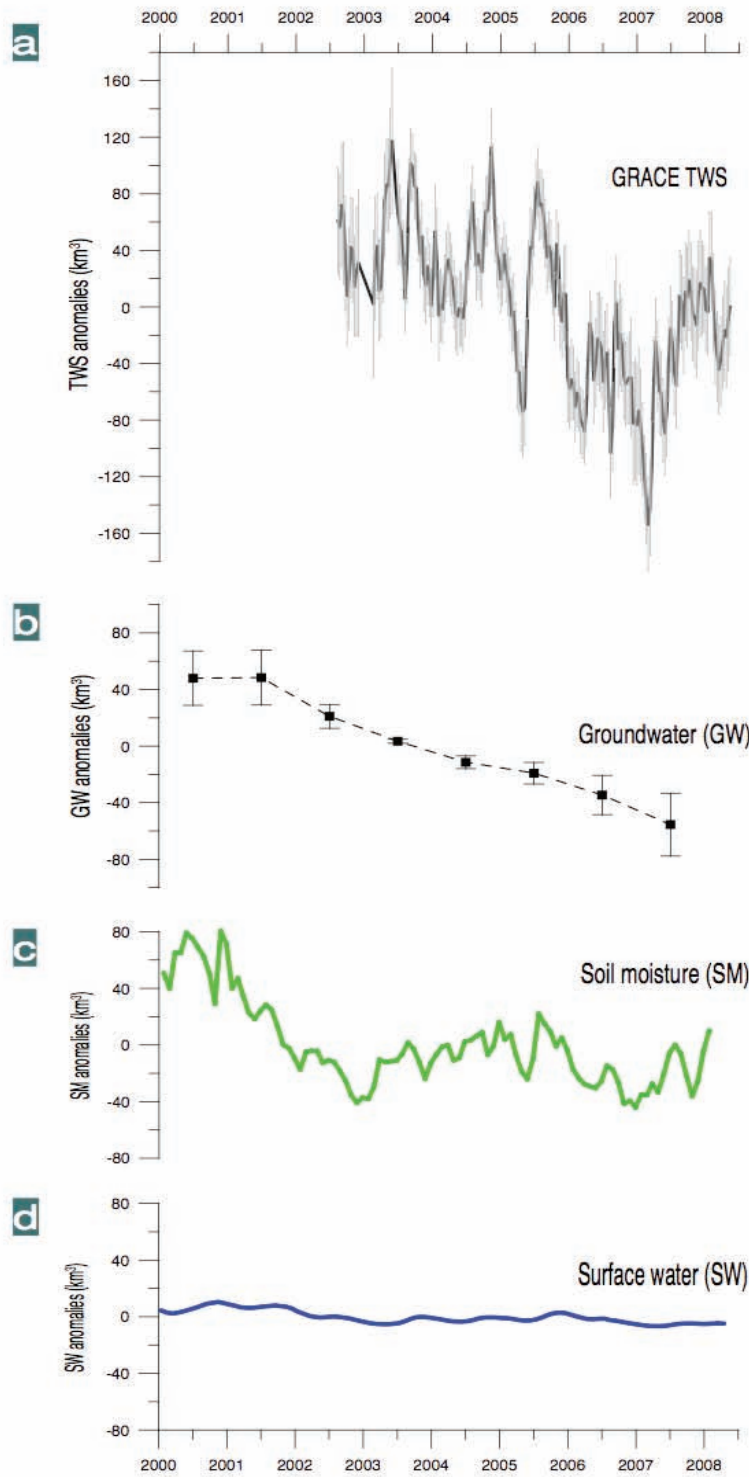


Figure 1. Change in water storage of the Murray-Darling Basin as estimated from a) GRACE space gravity observations b) groundwater borehole measurements c) GLDAS soil moisture model d) lake, river and reservoir level estimates (Leblanc et al., 2008)

A global dataset of frequency-dependent body-wave travel times: towards a global finite-frequency tomography of the Earth's mantle.

Christophe Zaroli¹, Eric Debayle¹ and Malcolm Sambridge²

¹ *Institut de Physique du Globe de Strasbourg, Ecole et Observatoire des Sciences de la Terre, Centre National de la Recherche Scientifique and Université de Strasbourg, France*

² *Research School of Earth Sciences, Australian National University, Canberra, ACT 0200, Australia*

With the growth in the number of seismic stations, the increase in computational power and the development of new analysis tools that extract more information from seismograms, the resolution of global seismic tomographic models has improved significantly in the last 25 years. For example the lateral resolution of surface wave velocity and anisotropy models of the upper mantle has decreased from 5000 km (Woodhouse and Dziewonski (1984), Nataf et al., 1984) to about 1000 km in the most recent seismic models, allowing the anisotropic behaviours between continents to be distinguished (Debayle et al., 2005).

Finite-frequency theory (Dahlen et al. 2000) incorporates single scattering into the formulation, and has been developed for long period body-waves. It is known that long period body waves are sensitive to the wave speed over a broad 3D volume surrounding the geometric ray. The corresponding 3D kernels have become known as "banana-doughnut" (BD) kernels because of their shape (See Figure 1).

The actual benefit of a finite-frequency theory remains controversial (Sieminski et al., 2004, de Hoop and van der Hilst, 2005a; Dahlen and Nolet, 2005; de Hoop and van der Hilst, 2005b; Montelli et al., 2006a; van der Hilst and de Hoop, 2006; Boschi et al., 2006). These authors suggest that the effect of the improved theory could be smaller than that of practical considerations such as the level of damping, the weighting of different data sets and the choice of data fit, especially when considering the relatively small amount of finite-frequency data (~90 000 long period body waves) compared with the large number (~1 500 000) of travel time data analysed with ray theory (e.g. van der Hilst et al. 2005).

Other limitations come from the travel-time datasets. Until now, most finite-frequency studies have been made using long period travel-times measured for ray theory applications. These travel times are not well suited for an inversion using Dahlen et al. (2000) kernels which are designed for travel-times measured by cross-correlation of a broadband seismic phase with a synthetic. To take a full advantage of Dahlen (2000) finite frequency theory, it is necessary to keep control of the frequency content of the waveform associated with a given travel-time, so that it can be associated with a finite-frequency kernel carrying the same frequency information. Secondly, by measuring finite frequency travel-times over different frequency ranges, it is possible to extract more information from each seismic phase. According to Dahlen et al., (2000), the width of a given BD kernel increases with the dominant period of the corresponding body waveform. Therefore, by measuring the travel-time of a seismic phase at several frequencies, there is a potential for increasing the amount of independent information in the inverse problem, as at each frequency, the waveform "senses" a different weighted average of the structure, through a different Banana Doughnut kernel.

If the debate about the real benefit of finite-frequency is still active, we believe that significant progress can be achieved by building a new dataset of massive long period body phases travel-times measured over a broad frequency range. To date, there is no such global database of frequency-dependent body-wave travel-time measurements.

A first result from this project is an automated approach for measuring long period body wave travel times at multiple frequencies. The approach has been designed to built a dataset for global finite-frequency SH or SV-wave tomography, but can be easily

extended to P-wave tomography. The travel times are computed by cross correlation and are fully compatible with the kernels provided by Dahlen, (2000). Currently, our approach allows us to measure in an automated way S, ScS, SS travel-times on SH components in different frequency-bands covering the period range 6–68 s. Frequency dependent crustal and attenuation corrections for WKBJ synthetics can also be incorporated.

The figures show the finite frequency kernels together with maps showing the coverage of the new data set. The automated procedure has been used to build a global dataset of finite frequency travel times, using 30 years of data from IRIS and GEOSCOPE networks. This will be the basis of future work on mantle imaging.

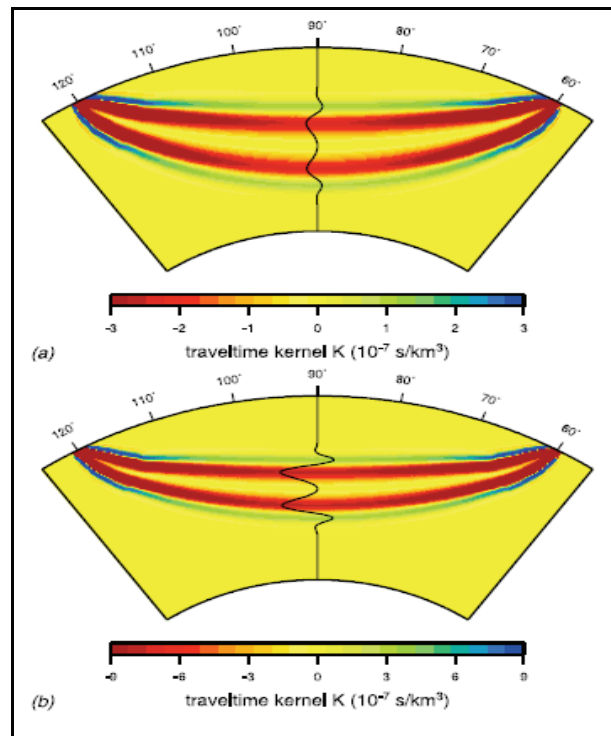


Figure 1. Fréchet Kernels at 20s period for a) P wave and b) S wave.

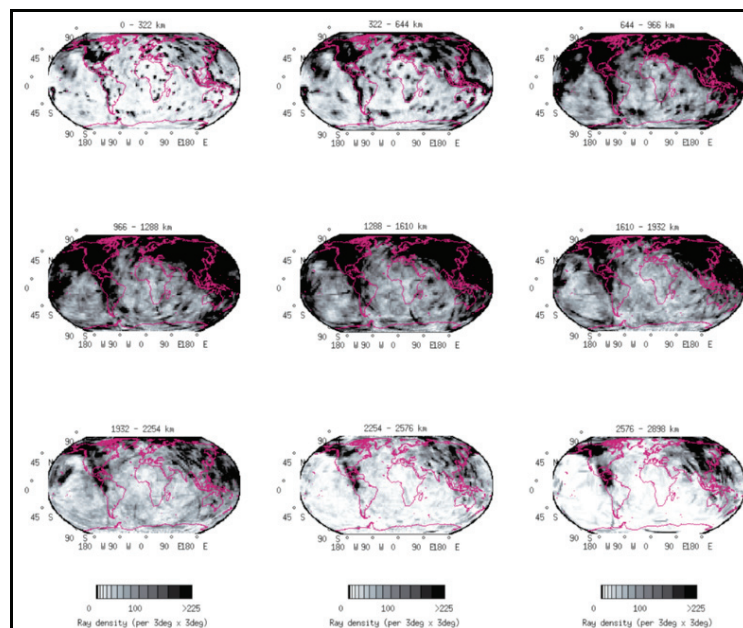


Figure 2. Ray density maps at different depth of the new dataset.

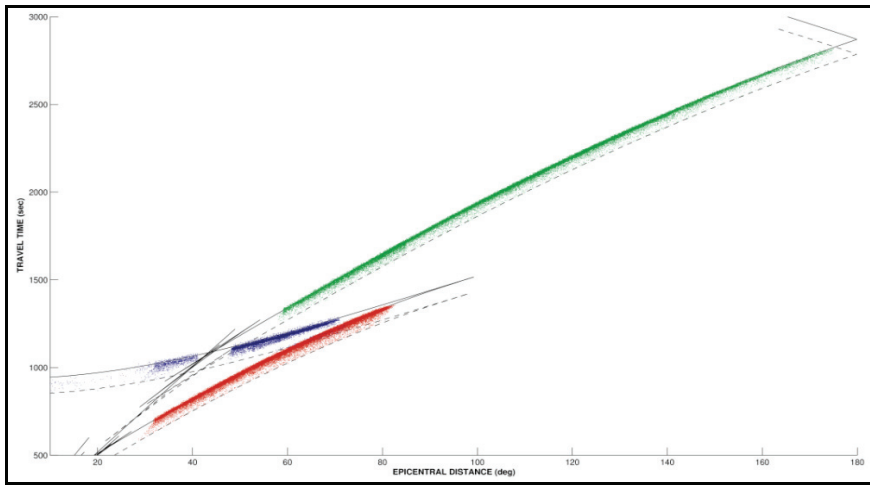


Figure 3. Arrival times of S, ScS and SS phases retained in the final dataset.

Australian trials of the French Transportable Laser Ranging System (FTLRS)

Jason Zhang¹, Chris Watson², Francis Pierron³,
Richard Coleman^{2,4,5}, Paul Tregoning¹

¹ Research School of Earth Sciences, Australian National University, Canberra, ACT

² University of Tasmania, Hobart, Tasmania

³ Observatoire de la Côte d'Azur, Grasse, France

⁴ Centre for Australian Weather and Climate Research (CAWCR), Hobart, Tasmania

⁵ Antarctic Climate and Ecosystems Cooperative Research Centre, Hobart, Tasmania

The Bass Strait in-situ calibration site has been used in the calibration and validation of satellite altimeter data since the launch of TOPEX/Poseidon in 1992. The primary focus at the site has been the estimation of absolute bias in altimeter derived sea surface height (SSH) using a combination of oceanographic moorings, GPS buoy deployments, coastal tide gauge and land based GPS data. As the sole site of its kind in the Southern Hemisphere, the Bass Strait site provides important input into understanding various error sources in satellite altimetry.

With an objective of improving our understanding of any geographically correlated orbit errors present in altimeter orbits, the Bass Strait site was selected as part of a collaborative French/Australian project to trial the French Transportable Laser Ranging System (FTLRS). The FTLRS was operated in Tasmania over a five month period between 1 December 2007 to 17 April 2008 jointly by French and Australian staff. The FTLRS and temporary GPS were located within the city of Burnie beneath Jason-1 descending pass 088, several kilometers from the Burnie tide gauge/CGPS and inland CGPS sites.

During the Tasmanian FTLRS campaign, a total of 673 overflights from 12 different satellites were observed and a total of 9200 normal points have been computed. In this poster, we present initial results from our analysis of FTLRS data. Whilst building SLR capacity in Australia, we seek to highlight the influence of an additional tracking station in this area of the Southern Hemisphere. Our FTLRS based orbits will assist in quantifying regional or geographically correlated orbit errors present in satellite altimeter data, allowing any bias in altimetry derived SSH in this region to be estimated.

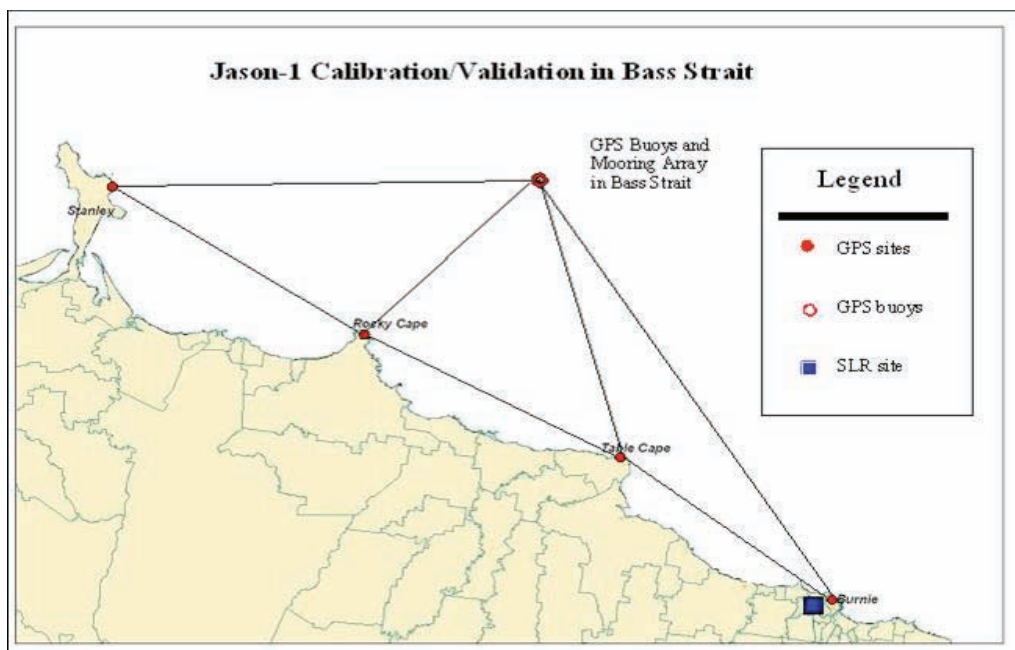


Figure 2. Sketch of the Bass Straite In-Situ Calibration Site

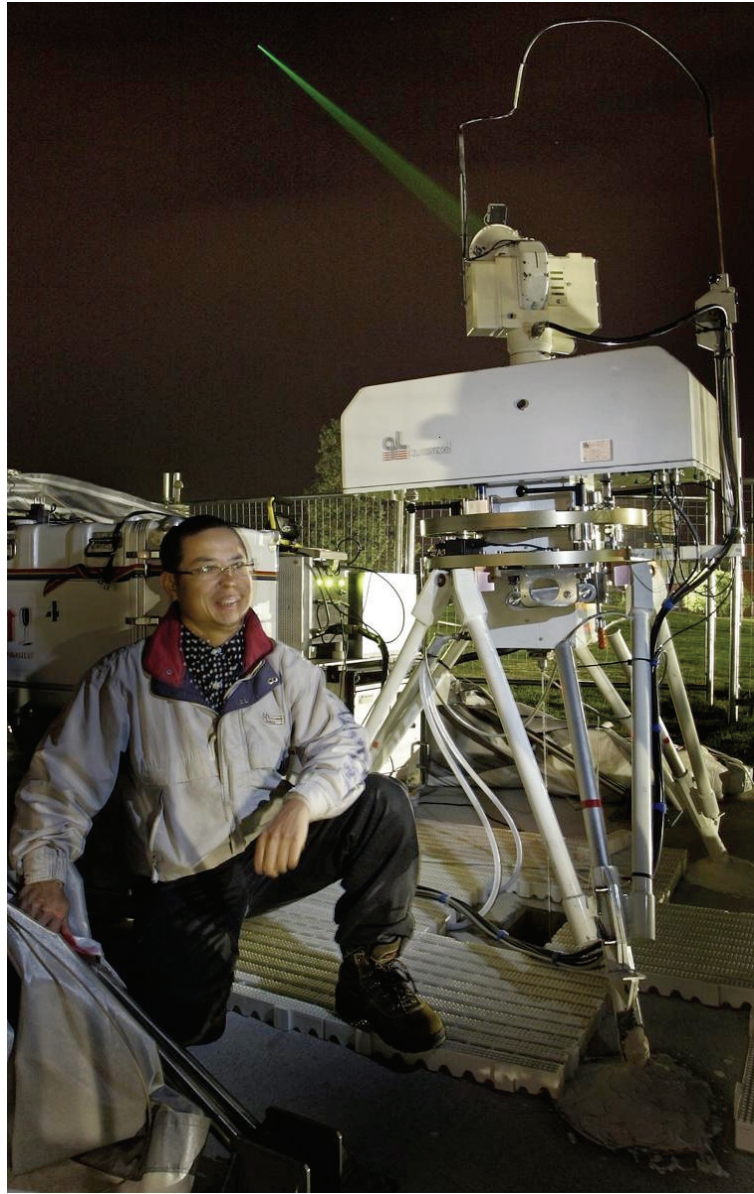


Figure 1. FTLRS in night operation